

Constrained Stochastic Recursive Momentum Successive Convex Approximation

Basil M. Idrees, Lavish Arora, and Ketan Rajawat

Abstract

We consider stochastic optimization problems with functional constraints, such as those arising in trajectory generation, sparse approximation, and robust classification. If the objective and constraint functions are not convex, the classical stochastic approximation algorithms such as the proximal stochastic gradient descent do not lead to efficient algorithms. The non-convex constraints in particular, are handled via penalty methods, primal-dual approaches, or within the successive convex approximation (SCA) rubric. Still, constrained optimization problems are thought to be harder than the unconstrained ones, and existing approaches for solving such problems cannot match the stochastic first order (SFO)-complexity lower bound for minimization of general smooth functions.

In this work, we put forth an accelerated SCA algorithm that utilizes the recursive momentum-based acceleration which is widely used in the unconstrained setting. Remarkably, the proposed algorithm also achieves the optimal SFO complexity, at par with that achieved by state-of-the-art (unconstrained) stochastic optimization algorithms. At each iteration, the proposed algorithm entails constructing convex surrogates of the objective and the constraint functions, and solving the resulting convex optimization problem. A recursive update rule is employed to track the gradient of the objective function, and contributes to achieving faster convergence and improved SFO complexity. A key ingredient of the proof is a new parameterized version of the standard Mangasarian-Fromowitz Constraints Qualification, that allows us to bound the dual variables and hence establish that the iterates approach an ϵ -stationary point. We also detail an obstacle-avoiding trajectory optimization problem that can be solved using the proposed algorithm, and show that its performance is superior to that of the existing algorithms. The performance of the proposed algorithm is also compared against that of a specialized sparse classification algorithm on a binary classification problem.

I. INTRODUCTION

A. Background

In this work, we consider the stochastic non-convex constrained optimization problem:

$$\begin{aligned}
 F^* &= \min_{\mathbf{x} \in \mathbb{R}^n} F(\mathbf{x}) := U(\mathbf{x}) + u(\mathbf{x}) & (\mathcal{P}) \\
 \text{s. t.} \quad & h_i(\mathbf{x}) \leq 0, & i = 1, \dots, I \\
 & g_j(\mathbf{x}) \leq 0, & j = 1, \dots, J
 \end{aligned}$$

where $U(\mathbf{x}) := \mathbb{E}[f(\mathbf{x}, \boldsymbol{\xi})]$ and f is a smooth possibly non-convex function, while $\{g_j\}_{j=1}^J$ are smooth but possibly non-convex functions. On the other hand, the functions $\{h_i\}_{i=1}^I$ are smooth convex functions, and u is a convex function. Here, the expectation is with respect to the random variable $\boldsymbol{\xi}$ with an unknown distribution. We seek to solve (\mathcal{P}) using stochastic approximation schemes that require independent samples of $\boldsymbol{\xi}$ observed sequentially over time.

Non-convex constrained optimization problems routinely arise in a number of areas, including robotics, machine learning, and signal processing. For instance, trajectory generation, target tracking, navigation, and path planning problems can often be cast as non-convex optimization problems [1]–[5] with non-convex obstacle-avoidance or boundary constraints. Similarly in supervised machine learning, constraints are often imposed ensure the resulting models are both robust and fair [6], [7]. Constraints may also be imposed to incorporate prior knowledge of the problem at hand, such as to ensure that the learned features are sparse in some domain [8].

Existing approaches to solve (\mathcal{P}) include the primal-dual method [9], penalty method [10], proximal point methods [11], [12], and several Successive Convex Approximation (SCA) variants [13]–[17]. The performance of these algorithms is usually measured in terms of their oracle complexity, which is the number of calls to the stochastic first-order (SFO) oracle required to reach a point that satisfies the Karush-Kuhn Tucher (KKT) conditions to within a tolerance of ϵ . The primal-dual method proposed in [9] iteratively updates both primal and dual variables based on a stochastic approximation to augmented Lagrangian function, achieving an oracle complexity of $\mathcal{O}(\epsilon^{-2.5})$. An improved rate of $\mathcal{O}(\epsilon^{-2})$ is achieved by [10] which utilizes a penalty functional to reformulate (\mathcal{P}) as an unconstrained optimization problem. The same rate is also achieved by the proximal point method ConEx [12] and level-constrained stochastic proximal gradient (LCSPG) method [11], both of which solve a sequence of strongly convex subproblems, obtained by adding

a quadratic term to the objective and constraint functions. A related level-constrained proximal point (LCPP) method [8] also achieved the same rate but was customized to only handle sparsity inducing constraint functions.

Different from these approaches, SCA represents a more flexible framework for solving generic non-convex constrained optimization problems. It is an iterative approach, where at every iteration, the non-convex objective and constraint functions are replaced with their convex surrogates, tailored to the problem at hand [18], [19]. Stochastic SCA variants have been proposed in [13]–[17], [20] for solving (\mathcal{P}) as well as its more general version with stochastic constraints. These works however only report asymptotic convergence results, and do not provide a comprehensive oracle complexity analysis. Non-asymptotic rates are only known for the classical SCA algorithm when solving the deterministic version of (\mathcal{P}) with convex constraints [21]–[24], where the latter work achieved the state-of-the-art rate of $\mathcal{O}(\epsilon^{-2})$.

We remark that the oracle complexity of $\mathcal{O}(\epsilon^{-2})$ achieved by various algorithms that solve (\mathcal{P}) is not optimum [25]. Indeed, using momentum or variance reduction techniques [26]–[30], it is well-known that the optimal oracle complexity of $\mathcal{O}(\epsilon^{-3/2})$ can be achieved for unconstrained or convex-constrained version of (\mathcal{P}) . Interestingly, variance reduction is applied to the level-constrained proximal algorithm in [11] for finite-sum problems but the rate achieved is only $\mathcal{O}(\epsilon^{-2})$, with a remark that it can be improved to $\mathcal{O}(\epsilon^{-3/2})$ if the objective is assumed to be smooth, but without any proof [11, Remark 5].

In this work, we incorporate STOchastic Recursive Momentum (STORM) updates from [26], [31] within the SCA framework to achieve the optimum rate of $\mathcal{O}(\epsilon^{-3/2})$. The proposed Constrained STORM SCA (CoSTA) algorithm uses momentum-enhanced surrogates with adaptive step-sizes in the spirit of [26], [31]. We also establish that the empirical performance of the proposed algorithm is better than that of CSSCA [13], which does not use momentum or variance-reduction, and at par with LCPP [8], which can only handle sparsity-inducing constraints.

Before concluding this section, we remark that analysis of optimization problems with non-convex constraints inevitably requires some assumptions called the constraint qualifications (CQ). These CQs are essential regularity conditions that ensure that the constraint functions are well-behaved, so that the intermediate updates or subproblems are well-defined. Technically, these CQs are utilized to ensure that the intermediate dual variables remain bounded across iterations. Commonly used CQs include the Non-singularity condition (NSC) [9], Linear Independence CQ (LICQ) [32], Linear Independence regularity condition (LIRC) [17], and most commonly

the Mangasarian-Fromovitz CQ (MFCQ) condition [8], [11], [12]. It was observed in [11, Sec. 3.1] that the classical MFCQ only implies the existence of a bound B on the dual variables, but does not relate B to the other problem parameters, leaving the possibility of B getting arbitrarily large. It was suggested in [11] to use a stronger CQ such as the strong feasibility CQ (SFCQ) so as to ensure a problem parameter-dependent oracle complexity bound. In this work, we instead utilize a stronger parameterized version of MFCQ to the same effect, i.e., bound the dual variables in terms of problem-dependent quantities.

Table I summarizes the comparative performance of various state-of-the-art algorithms that can be used to solve (\mathcal{P}) . We observe that the optimal rate is achieved only by the proposed CoSTA algorithm. Additional remarks on CQ and algorithm structure also included.

TABLE I: Comparison of the complexity results of several algorithms in literature to our algorithm to produce a stochastic ϵ -stationary solution of constrained stochastic non-convex optimization problem (To make the comparisons fair we have converted the oracle complexity results of the all the works to match our definition of (17)-(19))

Reference	Rate	Constraint Qualification	Remarks
CoSTA (This work)	$\mathcal{O}(\epsilon^{-3/2})$	Strong MFCQ	SCA-based
CSSCA [13], SSCA [15]	-	Slater's condition established for limit points	Asymptotic convergence proved
ConEx [12]	$\mathcal{O}(\epsilon^{-2})$	MFCQ / SFCQ	SCA-based
Stochastic Primal- Dual SGM [9]	$\mathcal{O}(\epsilon^{-2.5})$	NSC	Dual variables also updated
LCSPG [11]	$\mathcal{O}(\epsilon^{-2})$	MFCQ / SFCQ	Remark 5 mentions that improved rates are possible.
LCPP [8]	$\mathcal{O}(\epsilon^{-2})$	MFCQ	For sparsity-constrained problems only

B. Notations

The lower case letter are used for denoting scalars while bold lower case letters are used for denoting vectors. Also, bold upper case letters are used for denoting matrices. For a matrix \mathbf{A} , $\text{diag}(\mathbf{a})$ is used to denote diagonal matrix with elements (a_1, a_2, \dots, a_k) . We collect the functions $\{g_j\}_{j=1}^J$ and $\{h_i\}_{i=1}^I$ into vector-valued functions $\mathbf{g} : \mathbb{R}^n \rightarrow \mathbb{R}^J$ and $\mathbf{h} : \mathbb{R}^n \rightarrow \mathbb{R}^I$, respectively.

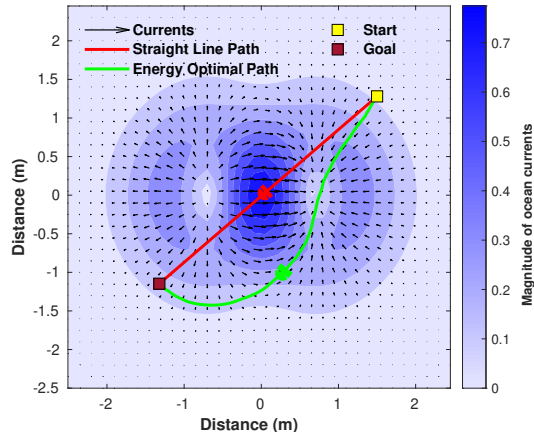


Fig. 1: Navigation under ocean currents. The green energy-optimal path harnesses the currents by judiciously applying control effort as the vehicle drifts along towards the goal, achieving lower energy (8.5 J) compared to the straight line path (14.8 J).

Binary operators such as \leq and \geq when applied to vectors are interpreted entry-wise, i.e., $\mathbf{g}(\mathbf{x}) \leq 0$ means $g_j(\mathbf{x}) \leq 0$ for all $1 \leq j \leq J$. We denote $\nabla \mathbf{g}(\mathbf{x}) = \left[\nabla g_1(\mathbf{x}) \ \dots \ \nabla g_J(\mathbf{x}) \right]^T$.

The rest of the paper is organized as follows. In Sec II we present an example that motivate the problem at hand. In Section III the problem statement is posed along with the proposed algorithm. In Section IV a non-asymptotic convergence analysis of the CoSTA algorithm is detailed. Section V briefly describes the potential application of CoSTA. Finally, Section VI the conclusion is provided.

II. MOTIVATING EXAMPLES

In this section, we discuss a variant of the widely studied Zermelo’s navigation problem [33], and formulate it as an instance of (\mathcal{P}) . Consider a surface vehicle in an ocean environment that seeks to traverse from one point to another, while using minimal energy. If the ocean currents are known ahead of time, the vehicle may save energy by moving along the flows instead of moving along the straight line from the source to the destination. An example is depicted in Fig. 1, where the straight line path (shown in red) incurs an energy of 14.8 J while the energy-optimal path (shown in green) requires only 8.5 J.

In practice however, the ocean currents in a given region $\mathcal{B} \subset \mathbb{R}^2$, denoted by $\vartheta(\mathbf{x})$ m/s for each $\mathbf{x} \in \mathcal{B}$, cannot be accurately predicted. Instead, various meteorological or oceanographic agencies [34]–[37] employ ensemble forecasting, a technique that captures the measurement uncertainty inherent to the prediction process, by providing a range of possible ocean current

forecasts [38], [39]. Mathematically, an instance of the ensemble forecast can be denoted by $\{\vartheta(\mathbf{x}, \boldsymbol{\xi})\}_{\mathbf{x} \in \mathcal{B}}$ where $\boldsymbol{\xi}$ is the index of a member of the ensemble. It has been observed that summary statistics, such as the average currents, cannot generally be used for path planning, as these may yield sub-optimal and potentially unsafe trajectories [40]. Instead, the ensemble forecasts should be directly employed to obtain trajectories that minimize the average energy.

In this work, we consider the problem of designing the energy-optimal trajectories of N agents, while avoiding an obstacle. Mathematically, the problem entails finding a collection of T waypoints $\{\mathbf{x}_i(\tau)\}_{\tau=1}^T$ for each agent i , collected in the super-vector $\underline{\mathbf{x}} \in \mathbb{R}^{2NT}$. The waypoints are equally spaced at intervals of $\Delta t = T_f/T$ seconds where T_f is the given time horizon. The i -th agent starts at a given location $\mathbf{x}_i(0)$ and wants to reach the goal location \mathbf{x}_i^g , such that $\mathbf{x}_i(T) = \mathbf{x}_i^g$. For collision avoidance, we assume that the agents and the obstacle have a circular shape with radii r and r^o , respectively. Finally, consider the agent's movement from $\mathbf{x}_i(\tau)$ to $\mathbf{x}_i(\tau + 1)$, where $0 \leq \tau \leq T - 1$. The control input — and consequently, the energy — can be considered proportional to the quantity $\|\mathbf{x}_i(\tau + 1) - \mathbf{x}_i(\tau) - \vartheta(\mathbf{x}_i(\tau), \boldsymbol{\xi})\Delta t\|^2$. Here, the term $\vartheta(\mathbf{x}_i(\tau), \boldsymbol{\xi})\Delta t$ approximates the vehicle's displacement without any control input. Hence, the vehicle should seek to minimize the cumulative energy input while ensuring that the magnitude of the control input does not exceed the vehicle specifications, denoted by v_i^{\max} . In summary, the considered problem can be written as

$$\min_{\underline{\mathbf{x}}} \sum_{i=1}^N \sum_{\tau=0}^{T-1} \mathbb{E}[\|\mathbf{x}_i(\tau + 1) - \mathbf{x}_i(\tau) - \vartheta(\mathbf{x}_i(\tau), \boldsymbol{\xi})\Delta t\|^2] \quad (1a)$$

$$\text{s. t. } \mathbf{x}_i(T) = \mathbf{x}_i^g \quad (1b)$$

$$\|\mathbf{x}_i(\tau) - \mathbf{x}^o\| \geq r^o + r, \quad \forall \tau, i \quad (1c)$$

$$\|\mathbf{x}_i(\tau) - \mathbf{x}_j(\tau)\| \geq 2r, \quad \forall \tau, i \neq j \quad (1d)$$

$$\|\mathbf{x}_i(\tau + 1) - \mathbf{x}_i(\tau) - \vartheta(\mathbf{x}_i(\tau), \boldsymbol{\xi})\Delta t\| \leq v_i^{\max} \Delta t \quad \forall \tau, i, \boldsymbol{\xi} \quad (1e)$$

where the objective seeks to minimize the cumulative energy consumption averaged over the given ensembles, (1b) enforces the termination condition, (1c)-(1d) ensure that the vehicles maintain safe distances from each other and from the obstacle, and (1e) limits the maximum control input for every agent, time, and realization. Of these, (1e) contains an impractically large number of constraints, one for each realization, and renders the problem difficult to solve. To avoid this issue, we consider a more stringent reformulation of the constraint that implies (1e). To this end, we assume that the ensemble forecasts have a uniformly bounded support, i.e.,

$\|\vartheta(\mathbf{x}, \boldsymbol{\xi}) - \mathbb{E}[\vartheta(\mathbf{x}, \boldsymbol{\xi})]\| \leq \Delta\vartheta^{\max}$ for $\mathbf{x} \in \mathcal{B}$. Introducing $\mathbb{E}[\vartheta(\mathbf{x}_i(\tau), \boldsymbol{\xi})] \Delta t$ inside the norm on the left of (1e) and using the triangle inequality, we observe that

$$\begin{aligned} & \|\mathbf{x}_i(\tau + 1) - \mathbf{x}_i(\tau) - \vartheta(\mathbf{x}_i(\tau), \boldsymbol{\xi})\Delta t\| \\ & \leq \|\mathbf{x}_i(\tau + 1) - \mathbf{x}_i(\tau) - \mathbb{E}[\vartheta(\mathbf{x}_i(\tau), \boldsymbol{\xi})] \Delta t\| \\ & \quad + \Delta t \|\vartheta(\mathbf{x}_i(\tau), \boldsymbol{\xi}) - \mathbb{E}[\vartheta(\mathbf{x}_i(\tau), \boldsymbol{\xi})]\| \\ & \leq \|\mathbf{x}_i(\tau + 1) - \mathbf{x}_i(\tau) - \mathbb{E}[\vartheta(\mathbf{x}_i(\tau), \boldsymbol{\xi})] \Delta t\| + \Delta\vartheta^{\max} \Delta t. \end{aligned} \quad (2)$$

Hence, the constraint

$$\|\mathbf{x}_i(\tau + 1) - \mathbf{x}_i(\tau) - \mathbb{E}[\vartheta(\mathbf{x}_i(\tau), \boldsymbol{\xi})] \Delta t\| \leq (v_i^{\max} - \Delta\vartheta^{\max})\Delta t \quad (3)$$

is the tightened version of (1e). It can be seen that if we design a trajectory that satisfies (3), then it would automatically satisfy (1e). However, the tightening might result in slightly sub-optimal trajectories. We can observe that the tightened problem (1a)-(1d),(3) admits the structure of (\mathcal{P}) and can be solved using the proposed algorithm.

III. PROPOSED ALGORITHM

This section describes the proposed CoSTA algorithm and states the assumptions necessary to analyze its complexity.

A. Problem

Let us revisit (\mathcal{P}) to re-write it in a more compact form and introduce the associated notation. Define

$$\mathcal{K} := \{\mathbf{x} \in \mathbb{R}^n \mid \mathbf{h}(\mathbf{x}) \leq 0\} \quad (4)$$

so that (\mathcal{P}) can be written as

$$\min_{\mathbf{x} \in \mathcal{K}} \mathbb{E}[f(\mathbf{x}, \boldsymbol{\xi})] + u(\mathbf{x}) \quad \text{s. t.} \quad \mathbf{g}(\mathbf{x}) \leq 0 \quad (\mathcal{P}')$$

The feasible region is given by $\mathcal{X} := \mathcal{K} \cap \{\mathbf{x} \in \mathbb{R}^n \mid \mathbf{g}(\mathbf{x}) \leq 0\}$ and the domain of (\mathcal{P}') is given by

$$\mathcal{D} = \text{dom}(F) \bigcap \bigcap_{j=1}^J \text{dom}(g_j) \bigcap \bigcap_{i=1}^I \text{dom}(h_i). \quad (5)$$

B. Proposed Algorithm

We now described the proposed successive convex optimization algorithm in detail. The algorithm is initialized at an arbitrary feasible point $\mathbf{x}_1 = \mathbf{x}_0 \in \mathcal{K}$ that satisfies $\mathbf{g}(\mathbf{x}_1) \leq 0$. At iteration t and given iterate \mathbf{x}_t , we construct a strongly convex and smooth surrogate $\hat{f}(\mathbf{x}, \mathbf{x}_t, \boldsymbol{\xi}_t)$ of the objective function $f(\mathbf{x}, \boldsymbol{\xi}_t)$ as well as smooth and convex surrogates $\{\tilde{g}_j(\mathbf{x}, \mathbf{x}_t)\}_{j=1}^J$ (collected into the vector-valued function $\tilde{\mathbf{g}}(\mathbf{x}, \mathbf{x}_t)$) of the constraint functions $\{g_j(\mathbf{x})\}_{j=1}^J$. These surrogates are subsequently used to formulate the following convex subproblem that must be solved at every iteration:

$$\begin{aligned} \hat{\mathbf{x}}_t &= \arg \min_{\mathbf{x} \in \mathcal{K}} \quad \tilde{f}(\mathbf{x}, \mathbf{x}_t, \mathbf{z}_t, \boldsymbol{\xi}_t) + u(\mathbf{x}) \\ &\text{s.t.} \quad \tilde{\mathbf{g}}(\mathbf{x}, \mathbf{x}_t) \leq 0 \end{aligned} \quad (\mathcal{P}_t)$$

where \tilde{f} is a *running* approximation of f , given by

$$\tilde{f}(\mathbf{x}, \mathbf{x}_t, \mathbf{z}_t, \boldsymbol{\xi}_t) := \hat{f}(\mathbf{x}, \mathbf{x}_t, \boldsymbol{\xi}_t) + (1 - \beta_t) \langle \mathbf{x} - \mathbf{x}_t, \mathbf{z}_t - \nabla f(\mathbf{x}_{t-1}, \boldsymbol{\xi}_t) \rangle \quad (6)$$

for some $\beta_t < 1$. Here, the auxiliary variable \mathbf{z}_t seeks to approximate $\nabla U(\mathbf{x}_t)$, and hence utilizes the gradient tracking update from [31]:

$$\mathbf{z}_{t+1} = \nabla f(\mathbf{x}_t, \boldsymbol{\xi}_t) + (1 - \beta_t)(\mathbf{z}_t - \nabla f(\mathbf{x}_{t-1}, \boldsymbol{\xi}_t)). \quad (7)$$

We can view \mathbf{z}_{t+1} as a convex combination of the unbiased gradient $\nabla f(\mathbf{x}_t, \boldsymbol{\xi}_t)$ and the variance-reduced gradient estimate $\mathbf{z}_t + \nabla f(\mathbf{x}_t, \boldsymbol{\xi}_t) - \nabla f(\mathbf{x}_{t-1}, \boldsymbol{\xi}_t)$ of SARAH [41], similar to the STORM update in [31] but different from the classical tracking rules used in [13], [24], [42]. Substituting (7) in (6), we see that $\tilde{f}(\mathbf{x}, \mathbf{x}_t, \mathbf{z}_t, \boldsymbol{\xi}_t) = \hat{f}(\mathbf{x}, \mathbf{x}_t, \boldsymbol{\xi}_t) + \langle \mathbf{x} - \mathbf{x}_t, \mathbf{z}_{t+1} - \nabla f(\mathbf{x}_t, \boldsymbol{\xi}_t) \rangle$. That is, the running approximation \tilde{f} comprises of the surrogate \hat{f} and an additional linear correction term that depends on the gradient tracking error. If the surrogate follows the tangent matching property, i.e., $\nabla \hat{f}(\mathbf{x}, \mathbf{x}, \boldsymbol{\xi}) = \nabla f(\mathbf{x}, \boldsymbol{\xi})$, then the update in (7) also implies that

$$\begin{aligned} &\nabla \tilde{f}(\mathbf{x}_t, \mathbf{x}_t, \mathbf{z}_t, \boldsymbol{\xi}_t) \\ &= \nabla \hat{f}(\mathbf{x}_t, \mathbf{x}_t, \boldsymbol{\xi}_t) + (1 - \beta_t)(\mathbf{z}_t - \nabla f(\mathbf{x}_{t-1}, \boldsymbol{\xi}_t)) \end{aligned} \quad (8)$$

$$= \nabla f(\mathbf{x}_t, \boldsymbol{\xi}_t) + (1 - \beta_t)(\mathbf{z}_t - \nabla f(\mathbf{x}_{t-1}, \boldsymbol{\xi}_t)) = \mathbf{z}_{t+1}. \quad (9)$$

Finally, we take a convex combination of $\hat{\mathbf{x}}_t$ obtained from (\mathcal{P}_t) and the current iterate \mathbf{x}_t to yield the next iterate:

$$\mathbf{x}_{t+1} = (1 - \eta_t)\mathbf{x}_t + \eta_t\hat{\mathbf{x}}_t. \quad (10)$$

for $\eta_t < 1$.

The choice of the step-size and momentum rules are similar to those in [31]. Specifically, define $G_t := \|\nabla f(\mathbf{x}_t, \boldsymbol{\xi}_t)\|$ so that

$$\eta_t := \frac{\bar{k}}{(w + \sum_{i=1}^t G_i^2)^{1/3}}, \quad \beta_{t+1} = c\eta_t^2 \quad (11)$$

with $\eta_0 = \frac{\bar{k}}{w^{1/3}}$. Such a choice adapts to the gradient norm and is known to reduce the bias as well as the variance of the resulting gradient estimate [27]. The CoSTA algorithm is summarized in Algorithm 1.

Algorithm 1 Constrained STORM Successive Convex Approximation (CoSTA) Algorithm

- 1: **Input:** Parameters \bar{k}, w, c , and feasible $\mathbf{x}_0 = \mathbf{x}_1 \in \mathcal{X}$,
 - 2: Initialize $\beta_1 := \frac{c\bar{k}^2}{w^{2/3}}$ and $\mathbf{z}_1 = \nabla f(\mathbf{x}_0, \boldsymbol{\xi}_1) = 0$
 - 3: **for** $t = 1$ **to** T **do**
 - 4: Update \mathbf{z}_{t+1} as per (7)
 - 5: Evaluate $\{\eta_t, \beta_{t+1}\}$ as per (11)
 - 6: Solve (\mathcal{P}_t) and update \mathbf{x}_{t+1} as per (10)
 - 7: **end for**
-

C. Assumptions

We discuss two classes of assumptions: those regarding the problem (\mathcal{P}) and those regarding the choice of the surrogate functions. The first set of assumptions can be viewed as restrictions on the classes of problems that are considered here, while the second set of assumptions restrict the design choices available to us when constructing surrogate functions and applying CoSTA to a given problem.

1) *Assumptions on (\mathcal{P}) :* Application of CoSTA requires (\mathcal{P}) to satisfy five key properties: problem should be well-defined on \mathcal{X} , initial \mathbf{x}_1 should be feasible, all functions should be smooth and Lipschitz-continuous, variance of the objective gradient should be bounded, and finally MFCQ.

A1. *The feasible set is subsumed by the domain set \mathcal{D} , i.e., $\mathcal{X} \subseteq \mathcal{D}$.*

A2. *The algorithm is initialized with a feasible \mathbf{x}_1 such that $F(\mathbf{x}_1) - F^* \leq B_1$.*

A3. The functions $f(\cdot, \boldsymbol{\xi})$, $\{g_j\}_{j=1}^J$, and $\{h_i\}_{i=1}^I$ are L -smooth and G -Lipschitz.

A4. The variances of the stochastic gradient components are bounded, i.e., $\mathbb{E}[\|\nabla f(\mathbf{x}, \boldsymbol{\xi}) - \nabla U(\mathbf{x})\|^2] \leq \sigma^2$ for all $\mathbf{x} \in \mathcal{X}$.

A5. All feasible points $\tilde{\mathbf{x}} \in \mathcal{X}$ satisfy the strong (ω, ρ) -MFCQ condition, implying that there exist $\omega \geq 0$ and $\rho > 0$ such that

$$\langle \nabla g_j(\tilde{\mathbf{x}}), \mathbf{d}_{\tilde{\mathbf{x}}} \rangle \leq -\rho \quad \forall j \in \bar{\mathcal{J}} := \{k \mid g_k(\tilde{\mathbf{x}}) \geq -\omega\} \quad (12a)$$

$$\langle \nabla h_i(\tilde{\mathbf{x}}), \mathbf{d}_{\tilde{\mathbf{x}}} \rangle \leq -\rho \quad \forall i \in \bar{\mathcal{I}} := \{l \mid h_l(\tilde{\mathbf{x}}) \geq -\omega\}. \quad (12b)$$

for some $\mathbf{d}_{\tilde{\mathbf{x}}} \in \mathbb{R}^n$ with $\|\mathbf{d}_{\tilde{\mathbf{x}}}\|_2 = 1$.

Assumptions **A1** and **A2** are standard and introduced to simplify the analysis. Implicit within **A2** is the requirement that F^* is bounded from below. The smoothness requirement in Assumption **A3** is again standard in the context of gradient-based algorithms. Note that Assumption **A3** implies that U is also L -smooth. The G -Lipschitz condition in Assumption **A3** implies that $G_t \leq G$ for all $t \geq 1$. Assumption **A4** is standard in the context of proximal stochastic gradient descent. A more relaxed version, where the gradient boundedness is only required at a specific point rather than at all points in \mathcal{X} has also been used in the literature [43], but its applicability to the non-convex constrained case remains an open problem. The MFCQ assumption in **A5** is critical and also common in the context of constrained optimization. The condition stems from the need to solve the convex optimization problem (\mathcal{P}_t) at every iteration. The subsequent analysis, as well as the analysis of most widely used convex optimization solvers, necessitates that Slater's condition be satisfied for the convex subproblem, primarily to ensure that the dual variables stay bounded. The MFCQ assumption on (\mathcal{P}) is required to ensure that Slater's condition holds for (\mathcal{P}_t) .

In the literature, the classical MFCQ condition, which corresponds to $\omega = 0$ and $\rho \rightarrow 0$, is commonly encountered, but is known to yield only asymptotic convergence results, as in [18]. This is because the classical MFCQ only implies that the dual variables associated with (\mathcal{P}_t) are bounded by an unknown parameter that may potentially depend on the solution path, as was also observed in [12, Remark 5]. However, the parameterized version of MFCQ in Assumption **A5** ensures that this bound is computable and depends solely on the initial conditions and the specific problem parameters such as L and ρ . Intuitively, the vector $\mathbf{d}_{\tilde{\mathbf{x}}}$ can be interpreted as a

direction along which one could move a sufficiently small distance, starting from $\tilde{\mathbf{x}}$, and stay feasible. We will formalize this intuition in Sec. IV and establish that Assumption **A5** implies the existence of a Slater point for (\mathcal{P}_t) . The existence of such a Slater point immediately yields a bound on the dual variables.

Before concluding, we remark that one could make stronger assumptions than MFCQ that may be easier to check in practice. For instance, [12] established non-asymptotic results under strong feasibility and compactness of the feasible region. In the present case however, strong feasibility of (\mathcal{P}) does not imply that Slater's condition holds for (\mathcal{P}_t) . Hence we do not pursue this approach.

2) *Assumption on surrogate functions:* We now describe the various assumptions that the surrogate functions must satisfy.

A6. For each $\mathbf{y} \in \mathcal{X}$, the surrogate $\hat{f}(\cdot, \mathbf{y}, \boldsymbol{\xi})$ satisfies:

- 1) *Strong convexity:* $\hat{f}(\cdot, \mathbf{y}, \boldsymbol{\xi})$ is μ -strongly convex;
- 2) *Smoothness:* $\hat{f}(\cdot, \mathbf{y}, \boldsymbol{\xi})$ is L -smooth; and
- 3) *Tangent match:* $\nabla \hat{f}(\mathbf{x}, \mathbf{y}, \boldsymbol{\xi}) = \nabla f(\mathbf{x}, \boldsymbol{\xi})$ for all $\mathbf{x} \in \mathcal{X}$.

A7. For each $\mathbf{y} \in \mathcal{X}$, the surrogates $\{\tilde{g}_j(\cdot, \mathbf{y})\}_{j=1}^J$ satisfy:

- 1) *Smoothness:* $\{\tilde{g}_j(\cdot, \mathbf{y})\}_{j=1}^J$ are L -smooth in \mathcal{X} ;
- 2) *Lipschitz continuity:* $\{\tilde{g}_j(\cdot, \mathbf{y})\}_{j=1}^J$ are G -Lipschitz in \mathcal{X} .
- 3) *Tangent match:* $\nabla \tilde{\mathbf{g}}(\mathbf{y}, \mathbf{y}) = \nabla \mathbf{g}(\mathbf{y})$;
- 4) *Upper bound:* $\mathbf{g}(\mathbf{x}) \leq \tilde{\mathbf{g}}(\mathbf{x}, \mathbf{y})$ for all $\mathbf{x} \in \mathcal{X}$ with equality at $\mathbf{x} = \mathbf{y}$.

A8. The surrogate $\tilde{f}(\cdot, \mathbf{y}, \mathbf{z}, \boldsymbol{\xi})$ is bounded over \mathcal{X} such that:

$$\tilde{f}(\cdot, \mathbf{y}, \mathbf{z}, \boldsymbol{\xi}) + u(\mathbf{x}) - \min_{\mathbf{x} \in \mathcal{X}(\mathbf{y})} (\tilde{f}(\cdot, \mathbf{y}, \mathbf{z}, \boldsymbol{\xi}) + u(\mathbf{x})) \leq B_U$$

where $\mathcal{X}(\mathbf{y}) := \mathcal{K} \cap \{\mathbf{x} \mid \tilde{\mathbf{g}}(\mathbf{x}, \mathbf{y}) \leq 0\} \subseteq \mathcal{X}$.

Assumptions **A6**, **A7**, and **A8** restrict the choice of the surrogate functions and have also been used in [13], [18]. Examples of surrogate functions satisfying Assumptions **A6**-**A7** can be found in [18], [44]. An implication of Assumptions **A3** and **A7** is that the function $\phi_j(\mathbf{x}) := g_j(\mathbf{x}) -$

$\tilde{g}_j(\mathbf{x}, \mathbf{x}_t)$ is $2L$ -smooth so that

$$\phi_j(\mathbf{x}) \leq \phi_j(\mathbf{x}_t) + \langle \nabla \phi_j(\mathbf{x}_t), \mathbf{x} - \mathbf{x}_t \rangle + L \|\mathbf{x} - \mathbf{x}_t\|^2 = L \|\mathbf{x} - \mathbf{x}_t\|^2 \quad (13)$$

$$\|\nabla \phi_j(\mathbf{x})\| = \|\nabla \phi_j(\mathbf{x}) - \nabla \phi_j(\mathbf{x}_t)\| \leq 2L \|\mathbf{x} - \mathbf{x}_t\| \quad (14)$$

for any $\mathbf{x} \in \mathcal{X}$.

Assumption **(A8)** is generally satisfied if \mathcal{X} is compact. In that case, since $\mathcal{X}(\mathbf{y}) \subseteq \mathcal{X}$, it follows that $\mathcal{X}(\mathbf{y})$ is compact for all \mathbf{y} . Since $\tilde{f}(\cdot, \mathbf{y}, \mathbf{z}, \boldsymbol{\xi})$ is a smooth and convex function, it is therefore bounded over the compact set $\mathcal{X}(\mathbf{y})$. In cases where \mathcal{X} is not compact, it may still be possible to satisfy Assumption **(A8)** by choosing the appropriate surrogate functions.

Before concluding the assumptions, the following remark regarding the problem parameters is due.

Remark 1. If $(0, \rho)$ -MFCQ holds for (\mathcal{P}) at $\tilde{\mathbf{x}} \in \mathcal{X}$ for some $\rho > 0$, then (ω, ρ) -MFCQ holds with

$$\omega = -\max\{\max_j g_j(\tilde{\mathbf{x}}), \max_i h_i(\tilde{\mathbf{x}})\}. \quad (15)$$

Further, given any ω , it is possible to ascertain ρ by solving the linear programming problem:

$$\begin{aligned} \max_{\rho, \mathbf{d}_{\tilde{\mathbf{x}}}} \quad & \rho & (16) \\ \text{s. t.} \quad & \langle \nabla g_j(\tilde{\mathbf{x}}), \mathbf{d}_{\tilde{\mathbf{x}}} \rangle \leq -\rho & \forall j \in \bar{\mathcal{J}} := \{j \mid g_j(\tilde{\mathbf{x}}) \geq -\omega\} \\ & \langle \nabla h_i(\tilde{\mathbf{x}}), \mathbf{d}_{\tilde{\mathbf{x}}} \rangle \leq -\rho & \forall i \in \bar{\mathcal{I}} := \{i \mid h_i(\tilde{\mathbf{x}}) \geq -\omega\}. \end{aligned}$$

In general however, determining global values of the different problem parameters σ , L , L_g , ω , and ρ may not be easy. In practice, the algorithm parameters are often tuned directly and without needing the problem parameters.

D. Approximate Optimality

The performance of the proposed algorithm will be studied in terms of its SFO complexity, i.e., the number of calls to the SFO oracle required to achieve an ϵ -KKT point in expectation.

Specifically, we characterize the number of SFO calls required by CoSTA to obtain a random feasible point $\tilde{\mathbf{x}} \in \mathcal{X}$, such that there exist $\tilde{\boldsymbol{\lambda}} \in \mathbb{R}_+^J$ and $\tilde{\boldsymbol{\nu}} \in \mathbb{R}_+^I$ with

$$\mathbb{E} \left[\left\| \nabla U(\tilde{\mathbf{x}}) + \nabla \mathbf{g}(\tilde{\mathbf{x}}) \tilde{\boldsymbol{\lambda}} + \nabla \mathbf{h}(\tilde{\mathbf{x}}) \tilde{\boldsymbol{\nu}} + \mathbf{v}_{\tilde{\mathbf{x}}} \right\| \right] \leq \sqrt{\epsilon}, \quad (17)$$

$$\mathbb{E} \left[\tilde{\boldsymbol{\lambda}}^\top \mathbf{g}(\tilde{\mathbf{x}}) \right] \geq -\epsilon \quad (18)$$

$$\mathbb{E} \left[\tilde{\boldsymbol{\nu}}^\top \mathbf{h}(\tilde{\mathbf{x}}) \right] \geq -\epsilon \quad (19)$$

for some $\mathbf{v}_{\tilde{\mathbf{x}}} \in \partial u(\tilde{\mathbf{x}})$. The definition of ϵ -KKT point for the stochastic case is an extension of its deterministic counterpart, first proposed in [45].

IV. COMPLEXITY ANALYSIS

In this section, we analyze the SFO complexity of the proposed algorithm. For the sake of brevity, we define for all $t \geq 1$:

$$\boldsymbol{\varepsilon}_t = \mathbf{z}_{t+1} - \nabla U(\mathbf{x}_t) \quad (\text{gradient tracking error}), \quad (20)$$

$$\boldsymbol{\delta}_t = \hat{\mathbf{x}}_t - \mathbf{x}_t, \quad (\text{iterate progress}) \quad (21)$$

$$\Delta_T = \frac{1}{T} \sum_{t=1}^T \mathbb{E} [\|\boldsymbol{\delta}_t\|] \quad (\text{average progress}). \quad (22)$$

The analysis proceeds as follows. Lemmas 1 and 2 establish recursive bounds the $\mathbb{E}[\|\boldsymbol{\varepsilon}_{t+1}\|^2]$ and $\mathbb{E}[F(\mathbf{x}_{t+1})]$ for each t . Lemma 3 proves the feasibility of iterates produced by the algorithm. Theorem 1 then uses these results to establish a bound on Δ_T . Next, Lemmas 4 and 5 respectively establish bound on primal and dual variables required for maintaining constraint feasibility under Assumption **A5**. Finally, Theorem 2 uses all these results to obtain the SFO complexity of CoSTA.

The results in Lemmas 1 and 2 follow from applying the results in [31] to SCA, but using a different metric $\mathbb{E}[\|\boldsymbol{\delta}_t\|^2]$ instead of $\mathbb{E}[\|\nabla U(\mathbf{x}_t)\|^2]$. The rate result in Theorem 1 also follows along similar lines. However, Lemmas 4 and 5 as well as Theorem 2 are entirely novel. The results also differ significantly from [13] where the focus is on non-asymptotic analysis.

Lemma 1. For all $t \geq 1$ and $\beta_{t+1} < 1$, it holds that

$$\frac{1}{16L^2} \mathbb{E} \left[\frac{\|\boldsymbol{\varepsilon}_{t+1}\|^2}{\eta_t(1-2\beta_{t+1})} \right] \leq \frac{1}{16L^2} \mathbb{E} \left[\frac{\|\boldsymbol{\varepsilon}_t\|^2}{\eta_t} \right] + \frac{\mathbb{E}[\eta_t \|\boldsymbol{\delta}_t\|^2]}{8} + \frac{1}{8L^2} \mathbb{E} \left[\frac{\beta_{t+1}^2 (G_{t+1})^2}{\eta_t(1-2\beta_{t+1})} \right]. \quad (23)$$

Lemma 1 provides a bound on gradient tracking error at the $(t+1)$ -th iteration in terms of the tracking error at t -th iteration as well as the iterate progress norm. The proof follows from expanding the left-hand side of (23) and introducing $(1-\beta_{t+1})\nabla U(\mathbf{x}_t)$. Subsequently, using the

smoothness of f , Assumption **A4**, and the definition of G_{t+1} , we obtain the desired bound. The full proof of this lemma is provided in Appendix A. Next we establish the descent lemma.

Lemma 2. The following inequality holds for $\mu \geq \frac{L\eta_t}{2} + \frac{3}{4}$:

$$\mathbb{E}[F(\mathbf{x}_{t+1}) - F(\mathbf{x}_t)] \leq \frac{\mathbb{E}[\eta_t \|\boldsymbol{\varepsilon}_t\|^2]}{2} - \frac{\mathbb{E}[\eta_t \|\boldsymbol{\delta}_t\|^2]}{4} \quad (24)$$

Lemma 2 bounds the change in F at every iteration. The proof of Lemma 2 starts with using the smoothness of U and the convexity of u . Subsequent use of the optimality condition of \mathcal{P}_t and Assumption **A6** yields the desired bound. The full proof of this lemma is provided in Appendix B. Next, we show that the choice of the surrogate functions \tilde{g}_j ensures that the iterates remain feasible for all $t \geq 1$.

Lemma 3. The iterates $\{\mathbf{x}_t\}_{t \geq 1}$ produced by Algorithm 1 are feasible for the original problem (\mathcal{P})

Proof: We use induction to establish the result. The algorithm is initialized with a feasible \mathbf{x}_1 . Suppose that $\mathbf{x}_t \in \mathcal{X}$ for some $t \geq 1$. Then, it can be seen that \mathbf{x}_t is feasible for (\mathcal{P}_t), i.e., $\mathbf{x}_t \in \mathcal{X}(\mathbf{x}_t)$. Further, since $\hat{\mathbf{x}}_t$ is the solution of (\mathcal{P}_t), it also satisfies $\hat{\mathbf{x}}_t \in \mathcal{X}(\mathbf{x}_t)$. Since \mathbf{x}_{t+1} is the convex combination of \mathbf{x}_t and $\hat{\mathbf{x}}_t$, and the set $\mathcal{X}(\mathbf{x}_t)$ is convex, it follows that $\mathbf{x}_{t+1} \in \mathcal{X}(\mathbf{x}_t)$. Finally, from Assumption **A7**, $\mathbf{g}(\mathbf{x}_{t+1}) \leq \tilde{\mathbf{g}}(\mathbf{x}_{t+1}, \mathbf{x}_t) \leq 0$, implying that $\mathbf{x}_{t+1} \in \mathcal{X}$. Therefore, by inductive hypothesis, \mathbf{x}_t is feasible for all $t \geq 1$. ■

We will now use Lemmas 1-3 to establish the following theorem which bounds the average error.

Theorem 1. If $0 < \bar{k} \leq w^{1/3}$, $\frac{w^{2/3}}{4k^2} \geq c \geq 4L^2 + \frac{G^2}{6Lk^3}$, and $w \geq \max\{(\frac{2L\bar{k}}{4\mu-3})^3, G^2\}$, then the following holds

$$\Delta_T \leq \sqrt{\frac{M_T(w + TG^2)^{1/3}}{T}} = \tilde{\mathcal{O}}\left(\frac{1}{T^{1/3}}\right) \quad (25)$$

where $M_T := 8B_1 + \frac{\sigma^2 w^{1/3}}{L^2 k^2} + \frac{2c^2 \bar{k}^2}{L^2} \log(T+2)$ and the $\tilde{\mathcal{O}}$ notation hides the dependence on logarithmic terms.

Proof: Since η_t is non-increasing, the bound on \bar{k} implies that $\eta_t \leq 1$ for all $t \geq 1$. We observe that since β_t is non-increasing and $c \leq \frac{w^{2/3}}{4k^2}$, it follows that $\beta_t \leq \beta_1 \leq \frac{1}{4}$ for all $t \geq 1$. Also, since η_t is non-increasing and $w \geq (\frac{2L\bar{k}}{4\mu-3})^3$, it follows that $\mu \geq \frac{L\eta_0}{2} + \frac{3}{4} \geq \frac{L\eta_t}{2} + \frac{3}{4}$, which is the required condition in Lemma 2.

Defining $\Psi_t = \mathbb{E}[F(\mathbf{x}_t) - F^*] + \frac{1}{16L^2} \mathbb{E}[\frac{\|\boldsymbol{\varepsilon}_t\|^2}{\eta_{t-1}(1-2\beta_t)}]$ and adding (23) with (24), we obtain

$$\Psi_{t+1} - \Psi_t \leq \mathbb{E} \left[\frac{\alpha_t}{16L^2} \|\boldsymbol{\varepsilon}_t\|^2 \right] - \frac{\mathbb{E}[\eta_t \|\boldsymbol{\delta}_t\|^2]}{8} + \frac{c^2}{8L^2} \mathbb{E} \left[\frac{\eta_t^3 G_{t+1}^2}{(1-2c\eta_t^2)} \right], \quad (26)$$

where $\alpha_t := 8L^2\eta_t + \frac{1}{\eta_t} - \frac{1}{(1-2\beta_t)\eta_{t-1}}$. In (26), we observe that the second term is already negative. We also want to select the algorithm parameters such that the first term is also non-positive, leaving the rate depending on the third term, which we will subsequently bound.

We first show that $\alpha_t \leq 0$. We begin with observing from concavity that since $(a+b)^{1/3} - a^{1/3} \leq \frac{b}{3a^{2/3}}$ for all $a, b \geq 0$, we have that

$$\frac{\bar{k}}{\eta_t} - \frac{\bar{k}}{\eta_{t-1}} = (w + \sum_{i=1}^t G_i^2)^{1/3} - (w + \sum_{i=1}^{t-1} G_i^2)^{1/3} \leq \frac{G_t^2}{3(w + \sum_{i=1}^{t-1} G_i^2)^{2/3}} = \frac{G_t^2 \eta_{t-1}^2}{3\bar{k}^2} \quad (27)$$

Therefore, we can simplify the first two terms in the definition of α_t by using (27) and the definition of β_t as

$$\frac{1}{\eta_t} - \frac{1}{(1-2\beta_t)\eta_{t-1}} = \frac{1}{\eta_t} - \frac{1}{\eta_{t-1}} - \frac{2\beta_t}{(1-2\beta_t)\eta_{t-1}} \leq \frac{G_t^2 \eta_{t-1}^2}{3\bar{k}^3} - \frac{2c\eta_{t-1}}{(1-2\beta_t)} \quad (28)$$

Finally, since $\eta_t \leq \eta_{t-1}$, $\beta_t > 0$, and $G_t \leq G$, we have that

$$\alpha_t = \frac{1}{\eta_t} - \frac{1}{(1-2\beta_t)\eta_{t-1}} + 8L^2\eta_t \stackrel{(28)}{\leq} \frac{G^2 \eta_{t-1}^2}{3\bar{k}^3} - 2c\eta_{t-1} + 8L^2\eta_{t-1} \quad (29)$$

$$= -2\eta_{t-1} \left(c - 4L^2 - \frac{G^2 \eta_{t-1}}{6\bar{k}^3} \right) \leq -2L^2 d \eta_{t-1} \quad (30)$$

where $d := \frac{1}{2L^2} (c - 4L^2 - \frac{G^2}{6\bar{k}^3}) > 0$. Therefore the first term on the right of (26) can be dropped.

For the second term on the right of (26), using the fact that $\eta_T \leq \eta_t$ as well as the Cauchy-Schwarz inequalities ($\mathbb{E}[XY]^2 \leq \mathbb{E}[X^2] \mathbb{E}[Y^2]$ for random variables X, Y and $\mathbf{1}^\top \mathbf{w} \leq \sqrt{T} \|\mathbf{w}\|$ for vector $\mathbf{w} \in \mathbb{R}^T$), we obtain

$$\mathbb{E} \left[\sum_{t=1}^T \eta_t \|\boldsymbol{\delta}_t\|^2 \right] \geq \mathbb{E} \left[\sum_{t=1}^T \eta_T \|\boldsymbol{\delta}_t\|^2 \right] \quad (31)$$

$$\geq \frac{1}{\mathbb{E}[1/\eta_T]} \mathbb{E} \left[\sqrt{\sum_{t=1}^T \|\boldsymbol{\delta}_t\|^2} \right]^2 \geq \frac{\bar{k}T \Delta_T^2}{(w + TG^2)^{1/3}}. \quad (32)$$

where we have used the fact that $\frac{1}{\eta_T} \leq \frac{1}{\bar{k}} (w + TG^2)^{1/3}$.

For the third term on the right of (26), we can use the fact that $w \geq G^2$ and the concavity of the log function as in [31, Lemma 4] to obtain

$$\begin{aligned} \sum_{t=1}^T \eta_t^3 G_{t+1}^2 &= \bar{k}^3 \sum_{t=1}^T \frac{G_{t+1}^2}{(w + \sum_{i=1}^t G_i^2)} \\ &\leq \bar{k}^3 \sum_{t=1}^T \frac{G_{t+1}^2}{(G^2 + \sum_{i=1}^{t+1} G_i^2)} \leq \bar{k}^3 \ln \left(1 + \sum_{t=1}^{T+1} \frac{G_t^2}{G^2} \right) \\ &\leq \bar{k}^3 \ln(T+2) \end{aligned} \quad (33)$$

Substituting (32) and (33) into (26), using the fact that $\beta_t \leq 1/4$, and summing over $t = 1, 2, \dots, T$, we obtain

$$\Psi_{T+1} - \Psi_1 \leq -\frac{\bar{k}T\Delta_T^2}{8(w + TG^2)^{1/3}} + \frac{c^2\bar{k}^3}{4L^2} \log(T+2) \quad (34)$$

Here, since $\mathbb{E}[\|\varepsilon_1\|^2] \leq \sigma^2$ from Assumption **A4**, we can bound

$$\Psi_1 \leq F(\mathbf{x}_1) - F^* + \frac{\sigma^2}{8L^2\eta_0}. \quad (35)$$

Further, the feasibility of \mathbf{x}_{T+1} as shown in Lemma 3 implies that $F^* \leq F(\mathbf{x}_{T+1})$ and hence $\Psi_{T+1} \geq 0$. Substituting into (34) and re-arranging, we obtain

$$\Delta_T^2 \leq M_T \frac{(w + TG^2)^{1/3}}{T} \quad (36)$$

where M_T is as defined in the statement of the theorem. ■

Corollary 1. If $0 < \bar{k} \leq w^{1/3}$, $\frac{w^{2/3}}{4k^2} \geq c > 4L^2 + \frac{G^2}{6Lk^3}$, and $w \geq \max\left\{\left(\frac{2L\bar{k}}{4\mu-3}\right)^3, G^2\right\}$, then it also holds that

$$\frac{1}{T} \sum_{t=1}^T \mathbb{E} [\|\delta_t\|^2] \leq \frac{M_T(w + TG^2)^{1/3}}{T} = \tilde{\mathcal{O}} \left(\frac{1}{T^{2/3}} \right) \quad (37a)$$

$$\frac{1}{T} \sum_{t=1}^T \mathbb{E} [\|\varepsilon_t\|] \leq \sqrt{\frac{M_T(w + TG^2)^{1/3}}{dT}} = \tilde{\mathcal{O}} \left(\frac{1}{T^{1/3}} \right) \quad (37b)$$

where $d = \frac{1}{2L^2}(c - 4L^2 - \frac{G^2}{6k^3})$.

The bound in (37a) of Corollary 1 can be established along the lines of Theorem 1 by lower bounding the RHS of (31) and using $\eta_T \leq \frac{\bar{k}}{(w+TG^2)^{1/3}}$. The bound in (37b) of Corollary 1 can be established on similar lines. Here, instead of dropping the first term on the right of (26), we drop the second term instead, and obtain a bound on the first term by proceeding along similar lines.

Theorem 1 and Corollary 1 establish bounds on the average tracking error and the average progress. These results will later be used to establish the required ϵ -KKT conditions and hence the SFO-complexity bound. To establish these bounds however, we need a strict feasibility condition, which will help us bound the dual variables corresponding to the t -th subproblem (\mathcal{P}_t) . This is where the MFCQ condition in Assumption **A5** enters into the picture.

Lemma 4. Under Assumption **A5**, there exists a strictly feasible $\tilde{\mathbf{x}}(\mathbf{x}_t) \in \mathcal{X}$ such that

$$\tilde{\mathbf{g}}(\tilde{\mathbf{x}}(\mathbf{x}_t), \mathbf{x}_t) \leq -\frac{\rho^2}{2L}. \quad (38)$$

$$\mathbf{h}(\tilde{\mathbf{x}}(\mathbf{x}_t)) \leq -\frac{\rho^2}{2L}. \quad (39)$$

where ρ is the parameter in Assumption (**A5**) for $\omega \geq \frac{\rho}{L}(G + \rho/2)$.

Lemma 4 implies that a strong version of Slater's constraint qualification holds for (\mathcal{P}_t) . In general, one cannot directly assume the existence of such as Slater point because the intermediate subproblems depend on \mathbf{x}_t which is generated by the algorithm. The proof of Lemma 4 is provided in Appendix C and follows from the smoothness and Lipschitz continuity properties of \tilde{g}_j and h_i .

Slater's constraint qualification together with the fact that $F^* > -\infty$ implies that strong duality holds for (\mathcal{P}_t) . Therefore, the primal-dual optimum solution, denoted by $(\hat{\mathbf{x}}_t, \hat{\boldsymbol{\lambda}}_t, \hat{\boldsymbol{\nu}}_t)$, satisfies the KKT conditions:

$$\tilde{\mathbf{g}}(\hat{\mathbf{x}}_t, \mathbf{x}_t) \leq 0, \mathbf{h}(\hat{\mathbf{x}}_t) \leq 0 \quad (40a)$$

$$\hat{\boldsymbol{\lambda}}_t \geq 0, \hat{\boldsymbol{\nu}}_t \geq 0 \quad (40b)$$

$$\hat{\boldsymbol{\lambda}}_t \odot \tilde{\mathbf{g}}(\hat{\mathbf{x}}_t, \mathbf{x}_t) = \hat{\boldsymbol{\nu}}_t \odot \mathbf{h}(\hat{\mathbf{x}}_t) = 0 \quad (40c)$$

where \odot denotes the Hadamard (entry-wise) product. Further, for some $\mathbf{v}_{\hat{\mathbf{x}}_t} \in \partial u(\hat{\mathbf{x}}_t)$, it holds that

$$\nabla \tilde{f}(\hat{\mathbf{x}}_t, \mathbf{x}_t, \mathbf{z}_t, \boldsymbol{\xi}_t) + \mathbf{v}_{\hat{\mathbf{x}}_t} + \nabla \tilde{\mathbf{g}}(\hat{\mathbf{x}}_t, \mathbf{x}_t) \hat{\boldsymbol{\lambda}}_t + \nabla \mathbf{h}(\hat{\mathbf{x}}_t) \hat{\boldsymbol{\nu}}_t = 0. \quad (40d)$$

The Slater's condition along with the boundedness assumption in **A8** allows us to bound the dual variables for each (\mathcal{P}_t) .

Lemma 5. For all $t \geq 1$, we have that $\|\hat{\boldsymbol{\lambda}}_t\|_1 + \|\hat{\boldsymbol{\nu}}_t\|_1 \leq \frac{2B_U L}{\rho^2}$.

To prove Lemma 5 we use the convexity of \tilde{f} , \tilde{g}_j , h_i , and u , as well as the results in Lemma 4 and Assumption **A8**. The proof of Lemma 5 is provided in Appendix D. Finally, we state the main result, which is regarding the existence of an ϵ -optimal KKT point.

Theorem 2. There exists some $1 \leq t \leq \tilde{O}(\epsilon^{-3/2})$ and $\hat{\lambda}_t \in \mathbb{R}_+^I$, $\hat{\nu}_t \in \mathbb{R}_+^J$ such that the point $(\hat{\mathbf{x}}_t, \hat{\lambda}_t, \hat{\nu}_t)$ is ϵ -KKT optimal.

Equivalently, Theorem 2 states that the point $(\hat{\mathbf{x}}_t, \hat{\lambda}_t, \hat{\nu}_t)$ for some $1 \leq t \leq T$ is ϵ -KKT optimal for $\epsilon = \tilde{O}(T^{-2/3})$. We provide the proof of Theorem 2, that relies on the results established in Theorem 1 and Lemma 5.

Proof: We with begin with establishing that $(\hat{\mathbf{x}}_t, \hat{\lambda}_t, \hat{\nu}_t)$ satisfies the approximate stationarity condition in (17) for some $1 \leq t \leq T$. Observe from (6) and (9) that

$$\nabla \tilde{f}(\hat{\mathbf{x}}_t, \mathbf{x}_t, \mathbf{z}_t, \boldsymbol{\xi}_t) = \nabla \hat{f}(\hat{\mathbf{x}}_t, \mathbf{x}_t, \boldsymbol{\xi}_t) + (1 - \beta_t)(\mathbf{z}_t - \nabla f(\mathbf{x}_{t-1}, \boldsymbol{\xi}_t)) \quad (41)$$

$$= \nabla \hat{f}(\hat{\mathbf{x}}_t, \mathbf{x}_t, \boldsymbol{\xi}_t) - \nabla \hat{f}(\mathbf{x}_t, \mathbf{x}_t, \boldsymbol{\xi}_t) + \mathbf{z}_{t+1} \quad (42)$$

Substituting in (40d) and re-arranging, we obtain

$$\mathbf{v}_{\hat{\mathbf{x}}_t} + \nabla \mathbf{h}(\hat{\mathbf{x}}_t) \hat{\nu}_t = -\nabla \tilde{\mathbf{g}}_j(\hat{\mathbf{x}}_t, \mathbf{x}_t) \hat{\lambda}_t - \nabla \hat{f}(\hat{\mathbf{x}}_t, \mathbf{x}_t, \boldsymbol{\xi}_t) + \nabla \hat{f}(\mathbf{x}_t, \mathbf{x}_t, \boldsymbol{\xi}_t) - \mathbf{z}_{t+1} \quad (43)$$

Adding $\nabla U(\hat{\mathbf{x}}_t) + \nabla \mathbf{g}(\hat{\mathbf{x}}_t) \hat{\lambda}_t$ to both sides, we obtain

$$\begin{aligned} & \nabla U(\hat{\mathbf{x}}_t) + \nabla \mathbf{g}_j(\hat{\mathbf{x}}_t) \hat{\lambda}_t + \nabla \mathbf{h}(\hat{\mathbf{x}}_t) \hat{\nu}_t + \mathbf{v}_{\hat{\mathbf{x}}_t} \\ &= \nabla U(\hat{\mathbf{x}}_t) - \mathbf{z}_{t+1} + \nabla \hat{f}(\mathbf{x}_t, \mathbf{x}_t, \boldsymbol{\xi}_t) - \nabla \hat{f}(\hat{\mathbf{x}}_t, \mathbf{x}_t, \boldsymbol{\xi}_t) \\ &+ \left(\nabla \mathbf{g}(\hat{\mathbf{x}}_t) - \nabla \tilde{\mathbf{g}}(\hat{\mathbf{x}}_t, \mathbf{x}_t) \right) \hat{\lambda}_t =: \boldsymbol{\pi}_t \end{aligned} \quad (44)$$

The norm of $\boldsymbol{\pi}_t$ can now be bounded using the triangle inequality. First note that since U is L -smooth, we have that

$$\begin{aligned} \|\nabla U(\hat{\mathbf{x}}_t) - \mathbf{z}_{t+1}\| &= \|\nabla U(\hat{\mathbf{x}}_t) - \nabla U(\mathbf{x}_t) + \nabla U(\mathbf{x}_t) - \mathbf{z}_{t+1}\| \\ &\leq L \|\hat{\mathbf{x}}_t - \mathbf{x}_t\| + \|\boldsymbol{\varepsilon}_t\| = L \|\boldsymbol{\delta}_t\| + \|\boldsymbol{\varepsilon}_t\| \end{aligned} \quad (45)$$

Likewise, since $\hat{f}(\cdot, \mathbf{x}_t, \boldsymbol{\xi}_t)$ is L -smooth from Assumption **A6**, it follows that

$\|\nabla \hat{f}(\mathbf{x}_t, \mathbf{x}_t, \boldsymbol{\xi}_t) - \nabla \hat{f}(\hat{\mathbf{x}}_t, \mathbf{x}_t, \boldsymbol{\xi}_t)\| \leq L \|\boldsymbol{\delta}_t\|$. Also from (14) and since $\hat{\lambda}_t \geq 0$, we have that

$$\left\| [\hat{\lambda}_t]_j (\nabla g_j(\hat{\mathbf{x}}_t) - \nabla \tilde{g}_j(\hat{\mathbf{x}}_t, \mathbf{x}_t)) \right\| \leq 2L [\hat{\lambda}_t]_j \|\hat{\mathbf{x}}_t - \mathbf{x}_t\| \quad (46)$$

and hence from the triangle inequality,

$$\begin{aligned} \left\| \left(\nabla \mathbf{g}(\hat{\mathbf{x}}_t) - \nabla \tilde{\mathbf{g}}(\hat{\mathbf{x}}_t, \mathbf{x}_t) \right) \hat{\boldsymbol{\lambda}}_t \right\| &\leq \sum_{j=1}^J \left\| [\hat{\boldsymbol{\lambda}}_t]_j (\nabla g_j(\hat{\mathbf{x}}_t) - \nabla \tilde{g}_j(\hat{\mathbf{x}}_t, \mathbf{x}_t)) \right\| \\ &\leq 2L \left\| \hat{\boldsymbol{\lambda}}_t \right\|_1 \|\hat{\mathbf{x}}_t - \mathbf{x}_t\|. \end{aligned} \quad (47)$$

Combining these bounds, we obtain

$$\|\boldsymbol{\pi}_t\| \leq 2L \left(1 + \frac{2B_U L}{\rho^2}\right) \|\boldsymbol{\delta}_t\| + \|\boldsymbol{\varepsilon}_t\| \quad (48)$$

Taking expectation and summing over all $t = 1, 2, \dots, T$, and using the bounds in Theorem 1 and Corollary 1, we obtain

$$\begin{aligned} \frac{1}{T} \sum_{t=1}^T \mathbb{E} [\|\boldsymbol{\pi}_t\|^2] &\leq \frac{2}{T} \sum_{t=1}^T \left(2L + \frac{4B_U L^2}{\rho^2}\right)^2 \mathbb{E} [\|\boldsymbol{\delta}_t\|^2] + \frac{2}{T} \sum_{t=1}^T \mathbb{E} [\|\boldsymbol{\varepsilon}_t\|^2] \\ &\leq \left(\left(2L + \frac{4B_U L^2}{\rho^2}\right)^2 + \frac{1}{d} \right) \frac{2M_T(w + TG^2)^{1/3}}{T} \\ &= \tilde{\mathcal{O}}(T^{-2/3}) \end{aligned} \quad (49)$$

$$= \tilde{\mathcal{O}}(T^{-2/3}) \quad (50)$$

Also note that,

$$\begin{aligned} \hat{\boldsymbol{\lambda}}_t^\top \mathbf{g}(\hat{\mathbf{x}}_t) &= \sum_{j=1}^J [\hat{\boldsymbol{\lambda}}_t]_j (\tilde{g}_j(\hat{\mathbf{x}}_t, \mathbf{x}_t) + g_j(\hat{\mathbf{x}}_t) - \tilde{g}_j(\hat{\mathbf{x}}_t, \mathbf{x}_t)) \\ &\stackrel{(40c)}{=} - \sum_{j=1}^J [\hat{\boldsymbol{\lambda}}_t]_j (\tilde{g}_j(\hat{\mathbf{x}}_t, \mathbf{x}_t) - g_j(\hat{\mathbf{x}}_t)) \end{aligned} \quad (51)$$

$$\stackrel{(13)}{\geq} -L \|\boldsymbol{\delta}_t\|^2 \sum_{j=1}^J [\hat{\boldsymbol{\lambda}}_t]_j \geq -\frac{2B_U L^2}{\rho^2} \|\boldsymbol{\delta}_t\|^2. \quad (52)$$

Taking expectation, summing over $t = 1, 2, \dots, T$, and using the bound in Corollary 1 we obtain,

$$\frac{1}{T} \sum_{t=1}^T \mathbb{E} [\hat{\boldsymbol{\lambda}}_t^\top \mathbf{g}(\hat{\mathbf{x}}_t)] \geq -\frac{2B_U L^2}{\rho^2} \frac{M_T(w + TG^2)^{1/3}}{T} = \tilde{\mathcal{O}}(T^{-2/3}). \quad (53)$$

Adding (50) with (53) and noting that since

$\min_{1 \leq t \leq T} (\mathbb{E} [\|\boldsymbol{\pi}_t\|^2] + \mathbb{E} [\hat{\boldsymbol{\lambda}}_t^\top \mathbf{g}(\hat{\mathbf{x}}_t)]) \leq \frac{1}{T} \sum_{t=1}^T \mathbb{E} [\|\boldsymbol{\pi}_t\|^2] + \frac{1}{T} \sum_{t=1}^T \mathbb{E} [\hat{\boldsymbol{\lambda}}_t^\top \mathbf{g}(\hat{\mathbf{x}}_t)]$, it follows that there exists $t \in \{1, \dots, T\}$ such that $\mathbb{E} [\|\boldsymbol{\pi}_t\|] \leq \sqrt{\epsilon}$ and $\mathbb{E} [\hat{\boldsymbol{\lambda}}_t^\top \mathbf{g}(\hat{\mathbf{x}}_t)] \geq -\epsilon$. Comparing with the required condition in (17) and (18), we can set $\epsilon = T^{-2/3}$. In other words, there exists some t such that the point $(\hat{\mathbf{x}}_t, \hat{\boldsymbol{\lambda}}_t, \hat{\boldsymbol{\nu}}_t)$ is approximately stationary and satisfies approximate complementary slackness.

For the same t , it already holds that $\hat{\boldsymbol{\lambda}}_t \geq 0, \hat{\boldsymbol{\nu}}_t \geq 0$ from (40b). Further, $\hat{\mathbf{x}}_t$ is also feasible for (\mathcal{P}) from (40a) and since $g_j(\hat{\mathbf{x}}_t) \leq \tilde{g}_j(\hat{\mathbf{x}}_t, \mathbf{x}_t) \leq 0$. Likewise, (19) already holds from (40c). ■

The SFO complexity bound of Theorem 2 matches the the SFO complexity of STORM [31], STORM+ [26] and Pstorm [29] for the unconstrained case. It is important to note that unlike STORM and Pstorm which were proposed for unconstrained problem and convex constrained problems respectively, our algorithm can handle non-convex constrains while achieving the same SFO complexity bound.

V. SIMULATIONS

In this section we will evaluate the numerical performance of CoSTA on the two problems. We will first discuss the classical problem of sparse binary classification and compare the performance of CoSTA with the Level-Constrained Proximal Point (LCPP) algorithm designed to handle non-convex sparse models [8]. Subsequently, we will discuss the implementation of CoSTA on the energy-optimal trajectory planning problem discussed in Sec. II.

A. Sparse Binary Classification

The problem of finding a sparse binary classifier can be written in the form of (\mathcal{P}') with the objective being the logistic loss function, i.e., $f(\mathbf{x}, \{\mathbf{a}, b\}) = \log(1 + e^{-b\mathbf{a}^T\mathbf{x}})$ and the constraint $g(\mathbf{x})$ taking form of a sparsity inducing function, such as the ℓ_1 norm or the minmax concave function [8]. The random variable here signifies the independent observations $\{\mathbf{a}, b\}$.

For our case we will take g to be minmax concave penalty (MCP) [8], given by:

$$g(\mathbf{x}) = \lambda\|\mathbf{x}\|_1 - \sum_{k=1}^n h_{\lambda,\theta}([\mathbf{x}]_k) \quad (54)$$

where $[\mathbf{x}]_k$ denotes the k -th entry of \mathbf{x} and $h_{\lambda,\theta}$ is defined as:

$$h_{\lambda,\theta}(x) = \begin{cases} \frac{x^2}{2\theta}, & |x| \leq \theta\lambda \\ \lambda|x| - \frac{\theta\lambda^2}{2}, & |x| > \theta\lambda. \end{cases} \quad (55)$$

We can obtain a smoothed version of the MCP by approximating $|x|$ as $\sqrt{x^2 + \varrho}$ where ϱ is a positive constant. Since the objective is already convex, its running surrogate \tilde{f} can be constructed using (6). On the other hand, the surrogate of $h_{\lambda,\theta}$ can be constructed as,

$$h_{\lambda,\theta}(x, x_t) = h_{\lambda,\theta}(x_t) + \nabla h_{\lambda,\theta}(x_t)(x - x_t) \quad (56)$$

$$= \begin{cases} \frac{x_t x}{\theta} - \frac{x_t^2}{2\theta}, & |x_t| \leq \theta\lambda \\ \frac{\lambda\varrho}{\sqrt{x_t^2 + \varrho}} - \frac{\theta\lambda^2}{2} + \frac{\lambda x_t x}{\sqrt{x_t^2 + \varrho}}, & |x_t| > \theta\lambda. \end{cases} \quad (57)$$

Hence, the surrogate of the constraint (54) at point \mathbf{x}_t becomes

$$g(\mathbf{x}, \mathbf{x}_t) = \lambda \|\mathbf{x}\|_1 - \sum_{k=1}^n h_{\lambda, \theta}([\mathbf{x}]_k, [\mathbf{x}_t]_k) \quad (58)$$

We compare the performance of our algorithm with that of the LCPP method, which was proposed in [8] for solving stochastic non-convex optimization problems with sparsity inducing non-convex constraints. It is proximal point algorithm that solves the a sequence of convex subproblems with gradually relaxed constraint levels.

TABLE II: Dataset Description

Datasets	Training size	Test Size	Dimentionality (n)
MNIST	60000	10000	784
gisette	6000	1000	5000

For our simulations use two datasets: MNIST and gisette, details of which are summarized in Table II. For the MNIST dataset, we consider the binary classification problem of classifying the handwritten digit 5 from the other digits. As the dataset consists of 10 classes this can be achieved by assigning a label +1 to digit 5 and -1 to other digits. Likewise, gisette dataset also consists handwritten digits, but here the classification is between the often confused digits 4 and 9.

For MCP we take $\lambda = 2$ and $\theta = 5$. The parameter values for LCPP are taken to be the same as those provided in [8]. The following CoSTA parameters were used after tuning them for best performance: (i) $\mu = 0.05, \bar{k} = 0.0051, c = 6 \times 10^5, w = 9000$ for gisette; and (ii) $\mu = 0.06, \bar{k} = 0.0018, c = 1.4 \times 10^6, w = 38000$ for MNIST.

Figs. 2a and 2b show the performance of CoSTA and LCPP for the MNIST and gisette datasets, respectively. We observe that the proposed CoSTA algorithm performs at par with LCPP for both the datasets. The classification performance is also summarized in Table III, where it can be seen that the test performance of CoSTA is always better than that of LCPP. These results are remarkable since CoSTA is a general-purpose non-convex optimization algorithm while LCPP is a customized algorithm for working with non-convex sparse models.

B. Energy-Optimal Trajectory Planning

Continuing the problem discussed in Sec. II, we apply CoSTA and CSSCA [13] to solve the energy-efficient trajectory planning problem (1)-(3) in a simulated 2D ocean environment. The

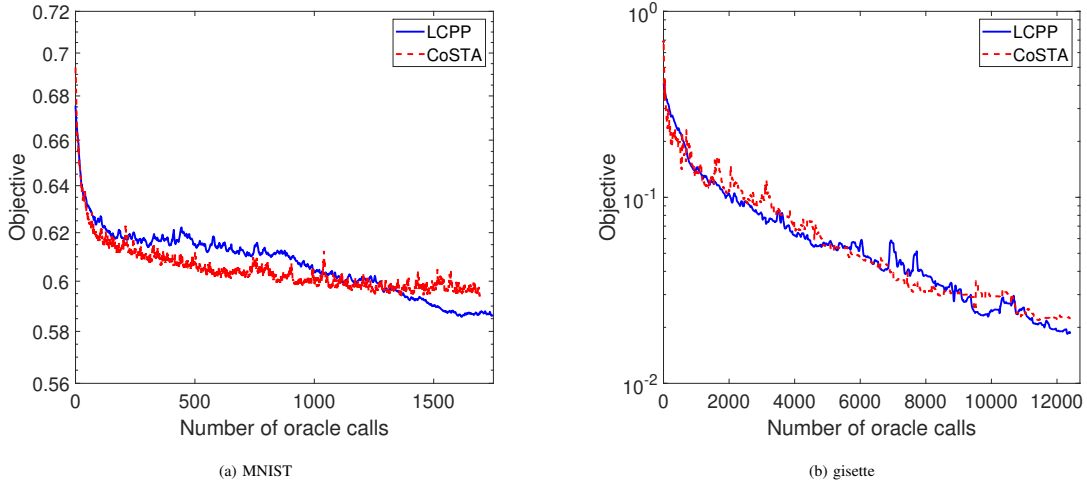


Fig. 2: Evolution of the objective function value across the number of calls to the oracle.

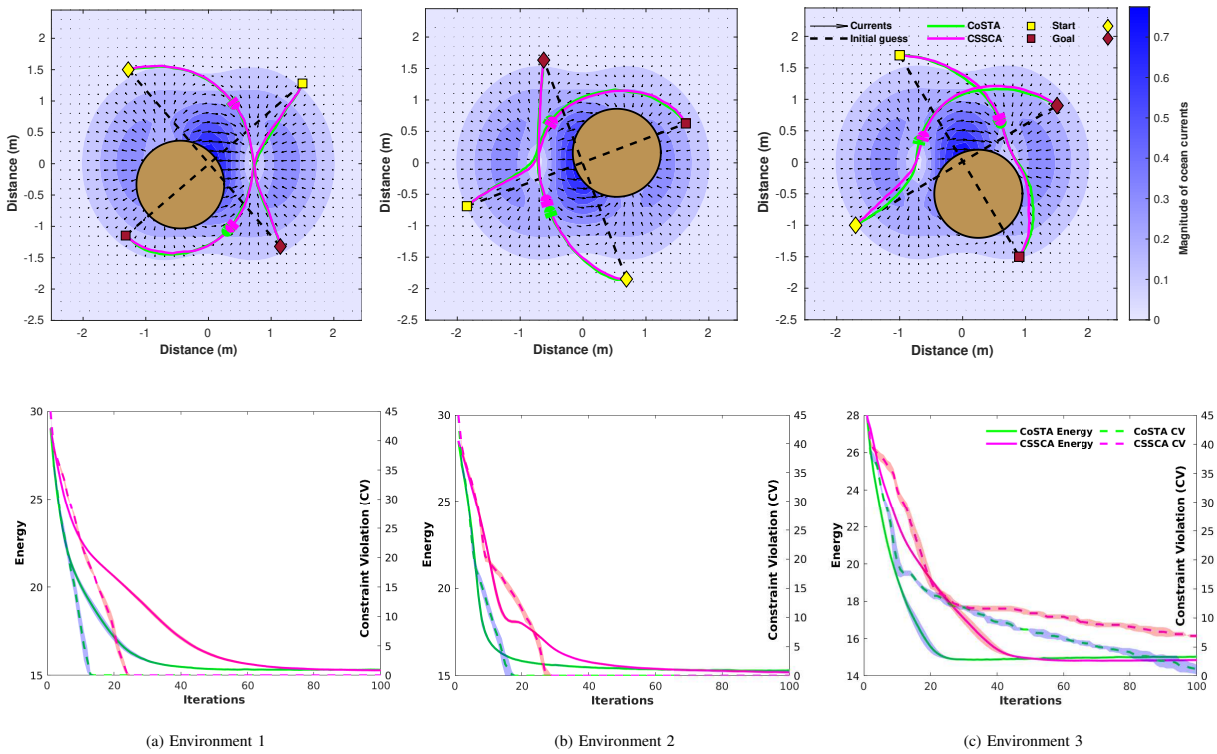
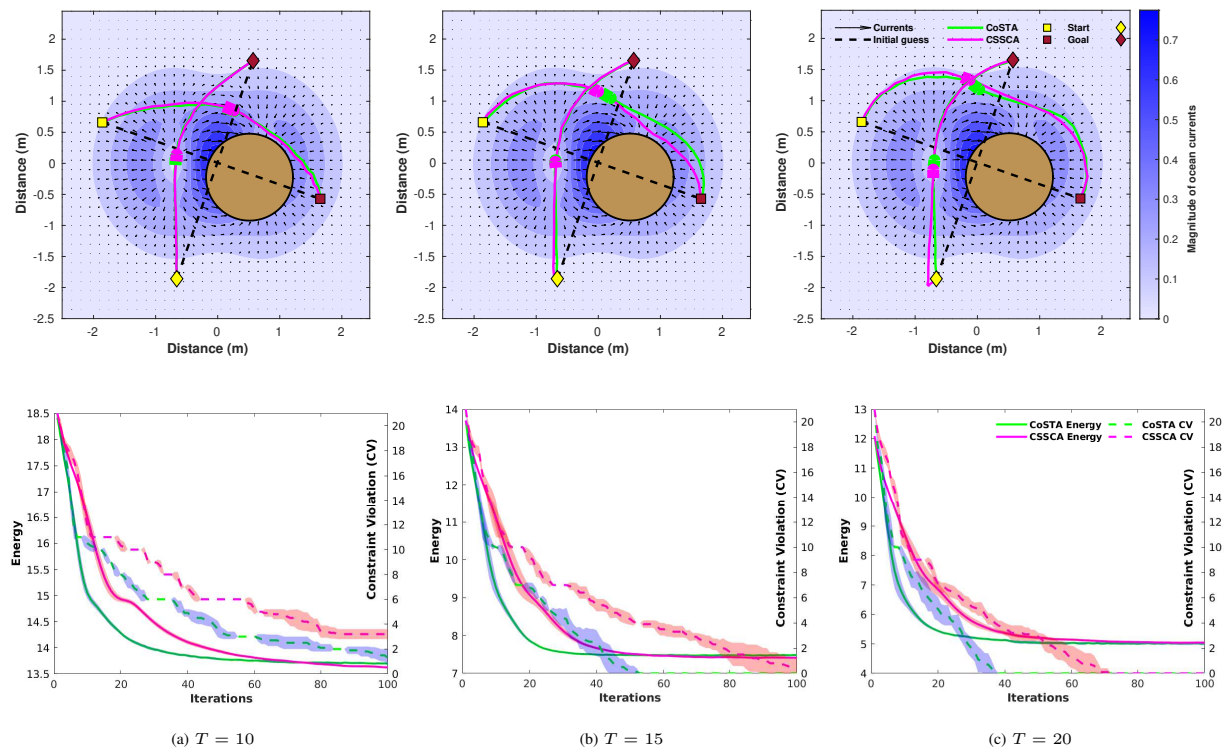


Fig. 3: Trajectory, energy, and mean constraint violation plots for $N = 60$, $T = 15$, and $\sigma = 0.2$, and environmental configurations 1, 2, and 3.

TABLE III: Classification accuracy of different algorithms for sparse logistic regression (where the entries are train accuracy/ test accuracy)

Dataset	Accuracy	LCPP	CoSTA
MNIST	train	90.5 ± 1.4	94 ± 0.56
	test	90.54 ± 1.51	94.1 ± 0.74
gisette	train	99.7 ± .05	99.44 ± 0.11
	test	97.36 ± 0.5	97.72 ± 0.32

Fig. 4: Trajectory, energy, and mean constraint violation plots for $N = 30$, $\sigma = 0.2$, environmental configuration 4, and different values of T .

ocean currents at a point $\mathbf{x} = [x_1 \ x_2]^T$ are simulated using the following equations

$$\vartheta(\mathbf{x}) = \omega \begin{bmatrix} 1 - 2x_1^2 \\ -2x_1x_2 \end{bmatrix} \exp\{-(x_1^2 + x_2^2)\}. \quad (59)$$

We generate current predictions by adding biased noise as follows:

$$\vartheta(\mathbf{x}, \boldsymbol{\xi}) = \vartheta(\mathbf{x})(\mathbf{I} + \text{diag}(\mathbf{e}(\boldsymbol{\xi}))), \quad (60)$$

where $\mathbf{e}(\boldsymbol{\xi}) \sim \mathcal{N}(\mathbf{0}, \sigma^2 \mathbf{I})$. As stated earlier, neither the true ocean currents nor the noise model is known to the vehicle, which can only query the predictor for noisy realizations $\vartheta(\mathbf{x}, \boldsymbol{\xi})$ of the currents.

We carry out Monte Carlo simulations for multiple environments consisting of two agents and an obstacle. Each environment has a different starting, goal, and obstacle locations. Of these, the third environment, shown in Fig. 3c is particularly challenging, as the ocean currents tend to push one of the agents into the obstacle, requiring more precise navigation. We also vary the values of number of way points N , mission time T , and the noise parameter σ , so as to compare the performance of the proposed CoSTA algorithm with that of CSSCA across diverse settings.

The parameters of CSSCA (μ , ρ , and γ [13]) and CoSTA (μ , \bar{k} , c , and w) were tuned for best possible performance after running the algorithms for initial 100 iterations. The results are averaged over 10 Monte Carlo runs for the following values of problem parameters: $\omega = 0.8$, $r^0 = 0.7\text{m}$, $r = 0.1\text{m}$, and $v_i^{\max} = 1\text{m/s}$ for $i \in \{1, 2\}$.

Fig. 3 shows the optimized trajectory of the agents along with energy and constraint violations for various environments and configurations. For each of the three environments depicted, both algorithms ultimately generate similar trajectories. However, CoSTA always converges faster, achieving the optimal energy and almost zero constraint violation in at most 30 iterations for environments 1 and 2. The convergence of both algorithms is slower on environment 3 as it is a more challenging one. For this environment CoSTA generates feasible trajectories for both the agents whereas CSSCA has non-zero constraint violation. These may be attributed to the adaptive step sizes in (11) of CoSTA unlike that of CSSCA, which allows our algorithm achieve a better progress towards an optimum.

Finally we plot trajectories and convergence plots for different mission times T in Fig. 4. When the mission times are larger, both the algorithms generate longer paths so as to leverage the additional time and obtain trajectories with lower energy. On the other hand, it can be observed in Fig. 4 that for $T = 10$, both the algorithms are unable to generate feasible trajectories within the stipulated 100 iterations. Hence, we conclude that higher mission times provide more flexibility to the algorithms so that they can generate feasible trajectories with zero constraint violation in fewer iterations. Finally, we observe the in all these cases, the proposed CoSTA algorithm converges faster than CSSCA.

VI. CONCLUSION

We have considered the problem of minimizing a stochastic non-convex optimization problem with non-convex constraints. While the problem has been well-studied, the state-of-the-art algorithms have suboptimal oracle complexity of $\mathcal{O}(\epsilon^{-2})$. We have proposed the CoSTA

algorithm that introduces recursive momentum updates, thereby achieving the unimprovable oracle complexity of $\mathcal{O}(\epsilon^{-3/2})$. The proposed algorithm is developed within the SCA framework, and requires convex surrogates of the objective and constraint functions at every iteration. We also introduced a parameterized version of the Mangasarian-Fromovitz constraint qualification that allows us to ensure that the intermediate subproblems are strictly feasible and the intermediate dual variable stay bounded, resulting in an oracle complexity bound that depends only on the problem parameters. Finally, the empirical performance of the proposed CoSTA algorithm is compared with the other state-of-the-art algorithms across two different applications: energy optimal trajectory design and sparse binary classification. The proposed algorithm outperforms the state-of-the-art algorithms on the energy optimal trajectory design problem and performs at par with the LCPP algorithm on the sparse binary classification problem.

APPENDIX A

PROOF OF LEMMA 1

Proof: The proof follows along the lines of [31, Lemma 2]. Expanding $\mathbf{z}_{t+1} - \nabla U(\mathbf{x}_t)$ from (7) and introducing $(1 - \beta_{t+1})\nabla U(\mathbf{x}_t)$, we obtain

$$\begin{aligned} \mathbf{z}_{t+2} - \nabla U(\mathbf{x}_{t+1}) &= (1 - \beta_{t+1})(\mathbf{z}_{t+1} - \nabla U(\mathbf{x}_t)) - (1 - \beta_{t+1})(\nabla f(\mathbf{x}_t, \boldsymbol{\xi}_{t+1}) - \nabla U(\mathbf{x}_t)) \\ &\quad + \nabla f(\mathbf{x}_{t+1}, \boldsymbol{\xi}_{t+1}) - \nabla U(\mathbf{x}_{t+1}) \end{aligned} \quad (61)$$

where observe that $\mathbb{E}_{\boldsymbol{\xi}_t}[\nabla U(\mathbf{x}_t) - \nabla f(\mathbf{x}_t, \boldsymbol{\xi}_{t+1})] = \mathbb{E}_{\boldsymbol{\xi}_t}[\nabla f(\mathbf{x}_{t+1}, \boldsymbol{\xi}_{t+1}) - \nabla U(\mathbf{x}_{t+1})] = 0$. Therefore, we have that

$$\begin{aligned} \mathbb{E}_{\boldsymbol{\xi}_{t+1}} \left[\frac{\|\mathbf{z}_{t+2} - \nabla U(\mathbf{x}_{t+1})\|^2}{\eta_t(1 - 2\beta_{t+1})} \right] &= \mathbb{E}_{\boldsymbol{\xi}_{t+1}} \left[\frac{(1 - \beta_{t+1})^2 \|\mathbf{z}_{t+1} - \nabla U(\mathbf{x}_t)\|^2}{\eta_t(1 - 2\beta_{t+1})} \right] \\ &\quad + \mathbb{E}_{\boldsymbol{\xi}_{t+1}} \left[\eta_t^{-1}(1 - 2\beta_{t+1})^{-1} \left\| (1 - \beta_{t+1})(\nabla f(\mathbf{x}_t, \boldsymbol{\xi}_{t+1}) \right. \right. \\ &\quad \left. \left. - \nabla U(\mathbf{x}_t) + \nabla U(\mathbf{x}_{t+1}) - \nabla f(\mathbf{x}_{t+1}, \boldsymbol{\xi}_{t+1}) \right) + \beta_{t+1}(\nabla f(\mathbf{x}_{t+1}, \boldsymbol{\xi}_{t+1}) - \nabla U(\mathbf{x}_{t+1})) \right\|^2 \right] \end{aligned} \quad (62)$$

where the cross term vanishes since $\mathbf{z}_{t+1} - \nabla U(\mathbf{x}_t)$ is independent of $\boldsymbol{\xi}_{t+1}$ and the second summand is zero mean. The second term in (62) can again be expanded as

$$\begin{aligned}
& \mathbb{E}_{\boldsymbol{\xi}_{t+1}} \left[\eta_t^{-1} (1 - 2\beta_{t+1})^{-1} \left\| (1 - \beta_{t+1}) (\nabla f(\mathbf{x}_t, \boldsymbol{\xi}_{t+1}) \right. \right. \\
& \quad \left. \left. - \nabla U(\mathbf{x}_t) + \nabla U(\mathbf{x}_{t+1}) - \nabla f(\mathbf{x}_{t+1}, \boldsymbol{\xi}_{t+1}) \right\|^2 \right] \\
& \quad + \beta_{t+1} \left\| \nabla f(\mathbf{x}_{t+1}, \boldsymbol{\xi}_{t+1}) - \nabla U(\mathbf{x}_{t+1}) \right\|^2 \\
& \stackrel{(a)}{\leq} 2\mathbb{E}_{\boldsymbol{\xi}_{t+1}} \left[\frac{(1 - \beta_{t+1})^2 \left\| \nabla f(\mathbf{x}_{t+1}, \boldsymbol{\xi}_{t+1}) - \nabla f(\mathbf{x}_t, \boldsymbol{\xi}_{t+1}) \right\|^2}{\eta_t (1 - 2\beta_{t+1})} \right] \\
& \quad + 2\mathbb{E}_{\boldsymbol{\xi}_{t+1}} \left[\frac{\beta_{t+1}^2 \left\| \nabla f(\mathbf{x}_{t+1}, \boldsymbol{\xi}_{t+1}) - \nabla U(\mathbf{x}_{t+1}) \right\|^2}{\eta_t (1 - 2\beta_{t+1})} \right] \\
& \stackrel{(b)}{\leq} 2\mathbb{E}_{\boldsymbol{\xi}_{t+1}} \left[\frac{(1 - \beta_{t+1})^2 \left\| \nabla f(\mathbf{x}_{t+1}, \boldsymbol{\xi}_{t+1}) - \nabla f(\mathbf{x}_t, \boldsymbol{\xi}_{t+1}) \right\|^2}{\eta_t (1 - 2\beta_{t+1})} \right] \\
& \quad + 2\mathbb{E}_{\boldsymbol{\xi}_{t+1}} \left[\frac{\beta_{t+1}^2 \left\| \nabla f(\mathbf{x}_{t+1}, \boldsymbol{\xi}_{t+1}) \right\|^2}{\eta_t (1 - 2\beta_{t+1})} \right] \tag{63}
\end{aligned}$$

where in (a) we have used the inequality $\mathbb{E}[\|X - \mathbb{E}[X] + Y\|^2] \leq 2\mathbb{E}[\|X\|^2] + 2\mathbb{E}[\|Y\|^2]$ for any random variables X and Y with bounded variances. And in (b) we have used $\mathbb{E}[\|X - \mathbb{E}[X]\|^2] \leq \mathbb{E}[\|X\|^2]$. Dividing both sides by $\frac{1}{16L^2}$, taking full expectation in (62) and using $\beta_{t+1} \leq 1$ (23) can be rewritten as,

$$\begin{aligned}
\frac{1}{16L^2} \mathbb{E} \left[\frac{\|\boldsymbol{\varepsilon}_{t+1}\|^2}{\eta_t (1 - 2\beta_{t+1})} \right] & \leq \frac{1}{16L^2} \mathbb{E} \left[\frac{\|\boldsymbol{\varepsilon}_t\|^2}{\eta_t} \right] + \frac{1}{8L^2} \mathbb{E} \left[\frac{\left\| \nabla f(\mathbf{x}_{t+1}, \boldsymbol{\xi}_{t+1}) - \nabla f(\mathbf{x}_t, \boldsymbol{\xi}_{t+1}) \right\|^2}{\eta_t} \right] \\
& \quad + \frac{1}{8L^2} \mathbb{E} \left[\frac{\beta_{t+1}^2 G_{t+1}^2}{\eta_t (1 - 2\beta_{t+1})} \right] \tag{64}
\end{aligned}$$

Using L -smoothness, and the update equation (10), we obtain

$$\begin{aligned}
\frac{1}{16L^2} \mathbb{E} \left[\frac{\|\boldsymbol{\varepsilon}_{t+1}\|^2}{\eta_t (1 - 2\beta_{t+1})} \right] & \leq \frac{1}{16L^2} \mathbb{E} \left[\frac{\|\boldsymbol{\varepsilon}_t\|^2}{\eta_t} \right] + \frac{1}{8} \mathbb{E} \left[\frac{\|\mathbf{x}_{t+1} - \mathbf{x}_t\|^2}{\eta_t} \right] + \frac{1}{8L^2} \mathbb{E} \left[\frac{\beta_{t+1}^2 G_{t+1}^2}{\eta_t (1 - 2\beta_{t+1})} \right] \\
& \leq \frac{1}{16L^2} \mathbb{E} \left[\frac{\|\boldsymbol{\varepsilon}_t\|^2}{\eta_t} \right] + \frac{1}{8} \mathbb{E} [\eta_t \|\boldsymbol{\delta}_t\|^2] + \frac{1}{8L^2} \mathbb{E} \left[\frac{\beta_{t+1}^2 G_{t+1}^2}{\eta_t (1 - 2\beta_{t+1})} \right]. \tag{65}
\end{aligned}$$

■

APPENDIX B

PROOF OF LEMMA 2

Proof: We first obtain a fundamental inequality. The optimality condition of (\mathcal{P}_t) implies that

$$\langle \mathbf{y} - \hat{\mathbf{x}}_t, \nabla \tilde{f}(\hat{\mathbf{x}}_t, \mathbf{x}_t, \mathbf{z}_t, \boldsymbol{\xi}_t) + \mathbf{v}_{\hat{\mathbf{x}}_t} \rangle \geq 0 \tag{66}$$

for all $\mathbf{y} \in \mathcal{X}(\mathbf{x}_t)$, where $\mathbf{v}_{\hat{\mathbf{x}}_t} \in \partial u(\hat{\mathbf{x}}_t)$. Choosing $\mathbf{y} = \mathbf{x}_t$,

$$\langle \mathbf{x}_t - \hat{\mathbf{x}}_t, \nabla \tilde{f}(\hat{\mathbf{x}}_t, \mathbf{x}_t, \mathbf{z}_t, \boldsymbol{\xi}_t) + \mathbf{v}_{\hat{\mathbf{x}}_t} \rangle \geq 0. \quad (67)$$

Adding and subtracting $\nabla \tilde{f}(\mathbf{x}_t, \mathbf{x}_t, \mathbf{z}_t, \boldsymbol{\xi}_t) = \mathbf{z}_{t+1}$, we obtain

$$\langle \hat{\mathbf{x}}_t - \mathbf{x}_t, \mathbf{z}_{t+1} + \mathbf{v}_{\hat{\mathbf{x}}_t} \rangle + \langle \hat{\mathbf{x}}_t - \mathbf{x}_t, \nabla \tilde{f}(\hat{\mathbf{x}}_t, \mathbf{x}_t, \mathbf{z}_t, \boldsymbol{\xi}_t) - \nabla \tilde{f}(\mathbf{x}_t, \mathbf{x}_t, \mathbf{z}_t, \boldsymbol{\xi}_t) \rangle \leq 0. \quad (68)$$

$$\Rightarrow \langle \mathbf{z}_{t+1} + \mathbf{v}_{\hat{\mathbf{x}}_t}, \hat{\mathbf{x}}_t - \mathbf{x}_t \rangle + \mu \|\hat{\mathbf{x}}_t - \mathbf{x}_t\|^2 \leq 0. \quad (69)$$

where we have used the strong monotonicity property of the gradient of the strongly convex function $\tilde{f}(\cdot, \mathbf{x}_t, \mathbf{z}_t, \boldsymbol{\xi}_t)$. From the convexity of u and the update rule (10), we obtain

$$u(\mathbf{x}_{t+1}) - u(\mathbf{x}_t) \leq \eta_t \langle \mathbf{v}_{\hat{\mathbf{x}}_t}, \hat{\mathbf{x}}_t - \mathbf{x}_t \rangle \quad (70)$$

Multiplying (69) by η_t and adding, we obtain

$$\eta_t \langle \mathbf{z}_{t+1}, \hat{\mathbf{x}}_t - \mathbf{x}_t \rangle \leq -\mu \eta_t \|\hat{\mathbf{x}}_t - \mathbf{x}_t\|^2 + u(\mathbf{x}_t) - u(\mathbf{x}_{t+1}). \quad (71)$$

Adding and subtracting $\nabla U(\mathbf{x}_t)$, we obtain

$$\begin{aligned} & \eta_t \langle \mathbf{z}_{t+1} - \nabla U(\mathbf{x}_t), \hat{\mathbf{x}}_t - \mathbf{x}_t \rangle + \eta_t \langle \nabla U(\mathbf{x}_t), \hat{\mathbf{x}}_t - \mathbf{x}_t \rangle \\ & \leq -\mu \eta_t \|\hat{\mathbf{x}}_t - \mathbf{x}_t\|^2 + u(\mathbf{x}_t) - u(\mathbf{x}_{t+1}) \end{aligned} \quad (72)$$

We now proceed to bound $U(\mathbf{x}_{t+1})$ in terms of $U(\mathbf{x}_t)$. Since U is smooth, we have that:

$$U(\mathbf{x}_{t+1}) \leq U(\mathbf{x}_t) + \langle \nabla U(\mathbf{x}_t), \mathbf{x}_{t+1} - \mathbf{x}_t \rangle + \frac{L}{2} \|\mathbf{x}_{t+1} - \mathbf{x}_t\|^2 \quad (73)$$

$$\leq U(\mathbf{x}_t) + \eta_t \langle \nabla U(\mathbf{x}_t), \hat{\mathbf{x}}_t - \mathbf{x}_t \rangle + \frac{L\eta_t^2}{2} \|\hat{\mathbf{x}}_t - \mathbf{x}_t\|^2 \quad (74)$$

$$\leq U(\mathbf{x}_t) + u(\mathbf{x}_t) - u(\mathbf{x}_{t+1}) - \eta_t \langle \mathbf{z}_{t+1} - \nabla U(\mathbf{x}_t), \hat{\mathbf{x}}_t - \mathbf{x}_t \rangle + \left(\frac{L}{2} \eta_t^2 - \mu \eta_t \right) \|\hat{\mathbf{x}}_t - \mathbf{x}_t\|^2 \quad (75)$$

where the last inequality follows from substituting (72). Using Young's inequality, rearranging, and taking expectation on both sides, we obtain

$$\begin{aligned} \mathbb{E}[F(\mathbf{x}_{t+1}) - F(\mathbf{x}_t)] & \leq \frac{1}{2} \mathbb{E} [\eta_t \|\nabla U(\mathbf{x}_t) - \mathbf{z}_{t+1}\|^2] \\ & \quad + \frac{L}{2} \mathbb{E} [\eta_t^2 \|\hat{\mathbf{x}}_t - \mathbf{x}_t\|^2] + \left(\frac{1}{2} - \mu \right) \eta_t \mathbb{E} [\|\hat{\mathbf{x}}_t - \mathbf{x}_t\|^2] \\ & \leq \frac{1}{2} \mathbb{E} [\eta_t \|\boldsymbol{\varepsilon}_t\|^2] - \frac{1}{4} \mathbb{E} [(4\mu - 2L\eta_t - 2)\eta_t \|\boldsymbol{\delta}_t\|^2] \end{aligned} \quad (76)$$

Finally, using $\mu > \frac{L\eta_t}{2} + \frac{3}{4}$, we get the desired result. \blacksquare

APPENDIX C

PROOF OF LEMMA 4

Proof: Since $\mathbf{x}_t \in \mathcal{X}$, strong MFCQ holds at \mathbf{x}_t , implying the existence of \mathbf{d}_t as specified in Assumption **(A5)**. Consider the point $\tilde{\mathbf{x}}(\mathbf{x}_t) = \mathbf{x}_t + \gamma \mathbf{d}_t$ for $\gamma > 0$ and let $\bar{\mathcal{I}}$ and $\bar{\mathcal{J}}$ be defined as the sets of indices corresponding to the near-active constraints at \mathbf{x}_t for the convex and general constraints, respectively.

First consider the near-active constraints at the feasible point \mathbf{x}_t . From the smoothness of $\tilde{g}_j(\cdot, \mathbf{x}_t)$, we have that

$$\tilde{g}_j(\tilde{\mathbf{x}}(\mathbf{x}_t), \mathbf{x}_t) \leq \tilde{g}_j(\mathbf{x}_t, \mathbf{x}_t) + \langle \nabla \tilde{g}_j(\mathbf{x}_t, \mathbf{x}_t), \tilde{\mathbf{x}}(\mathbf{x}_t) - \mathbf{x}_t \rangle + \frac{L}{2} \|\tilde{\mathbf{x}}(\mathbf{x}_t) - \mathbf{x}_t\|^2 \quad (77)$$

$$= \tilde{g}_j(\mathbf{x}_t) + \gamma \langle \nabla \tilde{g}_j(\mathbf{x}_t), \mathbf{d}_t \rangle + \frac{\gamma^2 L}{2} \leq -\rho\gamma + \frac{\gamma^2 L}{2} \quad (78)$$

for all $j \in \bar{\mathcal{J}}$. Likewise, from the smoothness of h_i , we have that

$$h_i(\tilde{\mathbf{x}}(\mathbf{x}_t)) \leq -\rho\gamma + \frac{\gamma^2 L}{2} \quad (79)$$

for all $i \in \bar{\mathcal{I}}$. Therefore, if we set $\gamma = \frac{\rho}{L}$, it can be seen that $\tilde{g}_j(\tilde{\mathbf{x}}(\mathbf{x}_t), \mathbf{x}_t) \leq -\frac{\rho^2}{2L}$ and $h_i(\tilde{\mathbf{x}}(\mathbf{x}_t)) \leq -\frac{\rho^2}{2L}$ as required. Since $\tilde{\mathbf{x}}(\mathbf{x}_t) \in \mathcal{X}$, it follows from Assumption **A1** that $\tilde{\mathbf{x}}(\mathbf{x}_t) \in \mathcal{D}$ and both the constraint functions are well-defined at $\tilde{\mathbf{x}}(\mathbf{x}_t)$.

Next, let us consider the strongly inactive constraints, where we have that

$$\tilde{g}_j(\tilde{\mathbf{x}}(\mathbf{x}_t), \mathbf{x}_t) = \tilde{g}_j(\tilde{\mathbf{x}}(\mathbf{x}_t), \mathbf{x}_t) - \tilde{g}_j(\mathbf{x}_t, \mathbf{x}_t) + g_j(\mathbf{x}_t) \quad (80)$$

$$\leq G \|\tilde{\mathbf{x}}(\mathbf{x}_t) - \mathbf{x}_t\| - \omega = \frac{G\rho}{L} - \omega \quad (81)$$

for all $j \notin \bar{\mathcal{J}}$, and likewise, from the Lipschitz continuity of h_i , we have that

$$h_i(\tilde{\mathbf{x}}(\mathbf{x}_t)) \leq \frac{G\rho}{L} - \omega \quad (82)$$

for all $i \notin \bar{\mathcal{I}}$. Therefore, the required condition is satisfied if we have $\omega \geq \frac{\rho}{L}(G + \rho/2)$. ■

APPENDIX D
PROOF OF LEMMA 5

Proof: Since $\tilde{f}(\cdot, \mathbf{x}_t, \mathbf{z}_t, \boldsymbol{\xi}_t)$, $\tilde{g}(\cdot, \mathbf{x}_t)$, and $h(\cdot)$ are convex functions, we have that for any $\mathbf{x} \in \mathcal{X}$,

$$\tilde{f}(\mathbf{x}, \mathbf{x}_t, \mathbf{z}_t, \boldsymbol{\xi}_t) + u(\mathbf{x}) \geq \tilde{f}(\hat{\mathbf{x}}_t, \mathbf{x}_t, \mathbf{z}_t, \boldsymbol{\xi}_t) + u(\hat{\mathbf{x}}_t) + \langle \nabla \tilde{f}(\hat{\mathbf{x}}_t, \mathbf{x}_t, \mathbf{z}_t, \boldsymbol{\xi}_t) + \mathbf{v}_{\hat{\mathbf{x}}_t}, \mathbf{x} - \hat{\mathbf{x}}_t \rangle \quad (83)$$

$$\tilde{g}_j(\mathbf{x}, \mathbf{x}_t) \geq \tilde{g}_j(\hat{\mathbf{x}}_t, \mathbf{x}_t) + \langle \nabla \tilde{g}_j(\hat{\mathbf{x}}_t, \mathbf{x}_t), \mathbf{x} - \hat{\mathbf{x}}_t \rangle \quad (84)$$

$$h_i(\mathbf{x}) \geq h_i(\hat{\mathbf{x}}_t) + \langle \nabla h_i(\hat{\mathbf{x}}_t), \mathbf{x} - \hat{\mathbf{x}}_t \rangle \quad (85)$$

for all $1 \leq j \leq J$ and $1 \leq i \leq I$. Setting $\mathbf{x} = \tilde{\mathbf{x}}(\mathbf{x}_t)$, multiplying (84) by $[\hat{\boldsymbol{\lambda}}_t]_j \geq 0$, multiplying (85) by $\nu_i(\hat{\mathbf{x}}_t)$, and adding with (83), we obtain

$$\begin{aligned} & \tilde{f}(\tilde{\mathbf{x}}(\mathbf{x}_t), \mathbf{x}_t, \mathbf{z}_t, \boldsymbol{\xi}_t) + u(\tilde{\mathbf{x}}(\mathbf{x}_t)) + \sum_{j=1}^J [\hat{\boldsymbol{\lambda}}_t]_j \tilde{g}_j(\tilde{\mathbf{x}}(\mathbf{x}_t), \mathbf{x}_t) + \sum_{i=1}^I \nu_i(\hat{\mathbf{x}}_t) h_i(\tilde{\mathbf{x}}(\mathbf{x}_t)) \\ & \geq \tilde{f}(\hat{\mathbf{x}}_t, \mathbf{x}_t, \mathbf{z}_t, \boldsymbol{\xi}_t) + u(\hat{\mathbf{x}}_t) + \sum_{j=1}^J [\hat{\boldsymbol{\lambda}}_t]_j \tilde{g}_j(\hat{\mathbf{x}}_t, \mathbf{x}_t) + \sum_{i=1}^I \nu_i(\hat{\mathbf{x}}_t) h_i(\hat{\mathbf{x}}_t) \\ & + \left\langle \sum_{j=1}^J [\hat{\boldsymbol{\lambda}}_t]_j \nabla \tilde{g}_j(\hat{\mathbf{x}}_t, \mathbf{x}_t) + \sum_{i=1}^I \nu_i(\hat{\mathbf{x}}_t) \nabla h_i(\hat{\mathbf{x}}_t) + \nabla \tilde{f}(\hat{\mathbf{x}}_t, \mathbf{x}_t, \mathbf{z}_t, \boldsymbol{\xi}_t) + \mathbf{v}_{\hat{\mathbf{x}}_t}, \hat{\mathbf{x}}_t - \tilde{\mathbf{x}}(\mathbf{x}_t) \right\rangle \end{aligned} \quad (86)$$

The last three terms on the right vanish from (40c) and (40d). So using Lemma 4, we have that

$$\begin{aligned} & \tilde{f}(\tilde{\mathbf{x}}(\mathbf{x}_t), \mathbf{x}_t, \mathbf{z}_t, \boldsymbol{\xi}_t) + u(\tilde{\mathbf{x}}(\mathbf{x}_t)) - \tilde{f}(\hat{\mathbf{x}}_t, \mathbf{x}_t, \mathbf{z}_t, \boldsymbol{\xi}_t) - u(\hat{\mathbf{x}}_t) \\ & \geq - \sum_{j=1}^J [\hat{\boldsymbol{\lambda}}_t]_j \tilde{g}_j(\tilde{\mathbf{x}}(\mathbf{x}_t), \mathbf{x}_t) - \sum_{i=1}^I \nu_i(\hat{\mathbf{x}}_t) h_i(\tilde{\mathbf{x}}(\mathbf{x}_t)) \end{aligned} \quad (87)$$

$$\geq \frac{\rho^2}{2L} \left(\sum_{j=1}^J [\hat{\boldsymbol{\lambda}}_t]_j + \sum_{i=1}^I \nu_i(\hat{\mathbf{x}}_t) \right). \quad (88)$$

Finally, using Assumption **(A8)** to upper bound the terms on the left, we obtain the desired result. ■

REFERENCES

- [1] J. Schulman, Y. Duan, J. Ho, A. Lee, I. Awwal, H. Bradlow, J. Pan, S. Patil, K. Goldberg, and P. Abbeel, "Motion planning with sequential convex optimization and convex collision checking," *The International Journal of Robotics Research*, vol. 33, no. 9, pp. 1251–1270, 2014.
- [2] D. Malyuta, T. P. Reynolds, M. Szmuk, T. Lew, R. Bonalli, M. Pavone, and B. Acikmese, "Convex optimization for trajectory generation: A tutorial on generating dynamically feasible trajectories reliably and efficiently," *IEEE Control Syst. Mag.*, vol. 42, no. 5, pp. 40–113, 2022.
- [3] T. A. Howell, B. E. Jackson, and Z. Manchester, "Altro: A fast solver for constrained trajectory optimization," in *2019 IEEE/RSJ International Conference on Intelligent Robots and Systems (IROS)*. IEEE, 2019, pp. 7674–7679.

- [4] O. Bounou, J. Ponce, and J. Carpentier, “Leveraging proximal optimization for differentiating optimal control solvers,” in *2023 62nd IEEE Conference on Decision and Control (CDC)*. IEEE, 2023, pp. 6313–6320.
- [5] W. Jallet, A. Bambade, N. Mansard, and J. Carpentier, “Constrained differential dynamic programming: A primal-dual augmented lagrangian approach,” in *2022 IEEE/RSJ International Conference on Intelligent Robots and Systems (IROS)*. IEEE, 2022, pp. 13 371–13 378.
- [6] S. T. Thomdapu, H. Vardhan, and K. Rajawat, “Stochastic compositional gradient descent under compositional constraints,” *IEEE Trans. Signal Process.*, vol. 71, pp. 1115–1127, 2023.
- [7] T. Chen, S. Barbarossa, X. Wang, G. B. Giannakis, and Z.-L. Zhang, “Learning and management for internet of things: Accounting for adaptivity and scalability,” *Proceedings of the IEEE*, vol. 107, no. 4, pp. 778–796, 2019.
- [8] D. Boob, Q. Deng, G. Lan, and Y. Wang, “A feasible level proximal point method for nonconvex sparse constrained optimization,” *Advances in Neural Information Processing Systems*, vol. 33, pp. 16 773–16 784, 2020.
- [9] L. Jin and X. Wang, “A stochastic primal-dual method for a class of nonconvex constrained optimization,” *Computational Optimization and Applications*, pp. 1–38, 2022.
- [10] X. Wang, S. Ma, and Y.-x. Yuan, “Penalty methods with stochastic approximation for stochastic nonlinear programming,” *Mathematics of computation*, vol. 86, no. 306, pp. 1793–1820, 2017.
- [11] D. Boob, Q. Deng, and G. Lan, “Level constrained first order methods for function constrained optimization,” *Mathematical Programming*, pp. 1–61, 2024.
- [12] —, “Stochastic first-order methods for convex and nonconvex functional constrained optimization,” *Mathematical Programming*, vol. 197, no. 1, pp. 215–279, 2023.
- [13] A. Liu, V. K. Lau, and B. Kananian, “Stochastic successive convex approximation for non-convex constrained stochastic optimization,” *IEEE Trans. Signal Process.*, vol. 67, no. 16, pp. 4189–4203, 2019.
- [14] A. Liu, V. K. Lau, and M.-J. Zhao, “Online successive convex approximation for two-stage stochastic nonconvex optimization,” *IEEE Trans. Signal Process.*, vol. 66, no. 22, pp. 5941–5955, 2018.
- [15] C. Ye and Y. Cui, “Stochastic successive convex approximation for general stochastic optimization problems,” *IEEE Wireless Commun. Lett.*, vol. 9, no. 6, pp. 755–759, 2019.
- [16] A. Liu, X. Chen, W. Yu, V. K. Lau, and M.-J. Zhao, “Two-timescale hybrid compression and forward for massive MIMO aided C-RAN,” *IEEE Trans. Signal Process.*, vol. 67, no. 9, pp. 2484–2498, 2019.
- [17] A. Liu, R. Yang, T. Q. Quek, and M.-J. Zhao, “Two-stage stochastic optimization via primal-dual decomposition and deep unrolling,” *IEEE Trans. Signal Process.*, vol. 69, pp. 3000–3015, 2021.
- [18] G. Scutari, F. Facchinei, and L. Lampariello, “Parallel and distributed methods for constrained nonconvex optimization—part I: Theory,” *IEEE Trans. Signal Process.*, vol. 65, no. 8, pp. 1929–1944, 2016.
- [19] G. Scutari, F. Facchinei, L. Lampariello, S. Sardellitti, and P. Song, “Parallel and distributed methods for constrained nonconvex optimization-part II: Applications in communications and machine learning,” *IEEE Trans. Signal Process.*, vol. 65, no. 8, pp. 1945–1960, 2016.
- [20] Y. Yang, G. Scutari, D. P. Palomar, and M. Pesavento, “A parallel decomposition method for nonconvex stochastic multi-agent optimization problems,” *IEEE Trans. Signal Process.*, vol. 64, no. 11, pp. 2949–2964, 2016.
- [21] A. Mokhtari, A. Koppel, G. Scutari, and A. Ribeiro, “Large-scale nonconvex stochastic optimization by doubly stochastic successive convex approximation,” in *IEEE ICASSP*, 2017, pp. 4701–4705.
- [22] A. Koppel, A. Mokhtari, and A. Ribeiro, “Parallel stochastic successive convex approximation method for large-scale dictionary learning,” in *IEEE ICASSP*, 2018, pp. 2771–2775.
- [23] A. Mokhtari and A. Koppel, “High-dimensional nonconvex stochastic optimization by doubly stochastic successive convex approximation,” *IEEE Trans. Signal Process.*, vol. 68, pp. 6287–6302, 2020.

- [24] B. M. Idrees, J. Akhtar, and K. Rajawat, “Practical precoding via asynchronous stochastic successive convex approximation,” *IEEE Trans. Signal Process.*, vol. 69, pp. 4177–4191, 2021.
- [25] Y. Arjevani, Y. Carmon, J. C. Duchi, D. J. Foster, N. Srebro, and B. Woodworth, “Lower bounds for non-convex stochastic optimization,” *Mathematical Programming*, vol. 199, no. 1, pp. 165–214, 2023.
- [26] K. Levy, A. Kavis, and V. Cevher, “Storm+: Fully adaptive sgd with momentum for nonconvex optimization,” in *35th Conference on Neural Information Processing Systems (NeurIPS 2021)*, no. CONF, 2021.
- [27] Q. Tran-Dinh, N. H. Pham, D. T. Phan, and L. M. Nguyen, “Hybrid stochastic gradient descent algorithms for stochastic nonconvex optimization,” *arXiv preprint arXiv:1905.05920*, 2019.
- [28] Z. Wang, K. Ji, Y. Zhou, Y. Liang, and V. Tarokh, “Spiderboost and momentum: Faster variance reduction algorithms,” *Advances in Neural Information Processing Systems*, vol. 32, 2019.
- [29] Y. Xu and Y. Xu, “Momentum-based variance-reduced proximal stochastic gradient method for composite nonconvex stochastic optimization,” *Journal of Optimization Theory and Applications*, vol. 196, no. 1, pp. 266–297, 2023.
- [30] N. H. Pham, L. M. Nguyen, D. T. Phan, and Q. Tran-Dinh, “ProxSARAH: An efficient algorithmic framework for stochastic composite nonconvex optimization,” *Journal of Machine Learning Research*, vol. 21, no. 110, pp. 1–48, 2020.
- [31] A. Cutkosky and F. Orabona, “Momentum-based variance reduction in non-convex SGD,” in *Advances in Neural Information Processing Systems*, 2019, pp. 15 236–15 245.
- [32] Q. Lin, R. Ma, and Y. Xu, “Complexity of an inexact proximal-point penalty method for constrained smooth non-convex optimization,” *Computational Optimization and Applications*, vol. 82, no. 1, pp. 175–224, 2022.
- [33] E. F. F. Zermelo, “Über das navigationsproblem bei ruhender oder veränderlicher windverteilung,” *Zamm-zeitschrift Fur Angewandte Mathematik Und Mechanik*, vol. 11, pp. 114–124, 1931. [Online]. Available: <https://api.semanticscholar.org/CorpusID:122686006>
- [34] “Ocean prediction - modelling for the future — world meteorological organization,” online, (Accessed on 12/04/2024). [Online]. Available: <https://public.wmo.int/en/resources/bulletin/ocean-prediction-modelling-future>
- [35] “Mercator ocean international,” online, (Accessed on 12/04/2024). [Online]. Available: <https://www.mercator-ocean.eu/en/>
- [36] “Copernicus marine service,” online, (Accessed on 12/04/2024). [Online]. Available: <https://marine.copernicus.eu/>
- [37] “Noaa tides & currents,” online, (Accessed on 12/04/2024). [Online]. Available: <https://tidesandcurrents.noaa.gov/ncop.html>
- [38] “A better way to study ocean currents — mit news — massachusetts institute of technology,” online, (Accessed on 12/04/2024). [Online]. Available: <https://news.mit.edu/2023/new-machine-learning-model-ocean-currents-0517>
- [39] T. Gneiting and A. E. Raftery, “Weather forecasting with ensemble methods,” *Science*, vol. 310, no. 5746, pp. 248–249, 2005.
- [40] C. Yoo, J. J. H. Lee, S. Anstee, and R. Fitch, “Path planning in uncertain ocean currents using ensemble forecasts,” in *2021 IEEE International Conference on Robotics and Automation (ICRA)*. IEEE, 2021, pp. 8323–8329.
- [41] L. M. Nguyen, J. Liu, K. Scheinberg, and M. Tak’avc, “Sarah a novel method for machine learning problems using stochastic recursive gradient,” in *International Conference on Machine Learning*. PMLR, 2017, pp. 2613–2621.
- [42] A. Mokhtari, H. Hassani, and A. Karbasi, “Stochastic conditional gradient methods: From convex minimization to submodular maximization,” *The Journal of Machine Learning Research*, vol. 21, no. 1, pp. 4232–4280, 2020.
- [43] A. Khaled, O. Sebbouh, N. Loizou, R. M. Gower, and P. Richtárik, “Unified analysis of stochastic gradient methods for composite convex and smooth optimization,” *Journal of Optimization Theory and Applications*, vol. 199, no. 2, pp. 499–540, 2023.
- [44] Y. Sun, P. Babu, and D. P. Palomar, “Majorization-minimization algorithms in signal processing, communications, and machine learning,” *IEEE Trans. Signal Process.*, vol. 65, no. 3, pp. 794–816, 2016.

- [45] J. Dutta, K. Deb, R. Tulshyan, and R. Arora, "Approximate KKT points and a proximity measure for termination," *Journal of Global Optimization*, vol. 56, no. 4, pp. 1463–1499, 2013.